2017

Electrochemical Sensor for Metal Ions and Phosphate Ion Detection for Biomedical and Agriculture Application

Md Faisal Kabir
South Dakota State University

ELECTROCHEMICAL SENSOR FOR METAL IONS AND PHOSPHATE ION DETECTION FOR BIOMEDICAL AND AGRICULTURE APPLICATION

BY

MD FAISAL KABIR

A thesis submitted in partial fulfillment of the requirements for the

Master of Science

Major in Electrical Engineering

South Dakota State University

2017

ELECTROCHEMICAL SENSOR FOR METAL IONS AND PHOSPHATE ION DETECTION FOR BIOMEDICAL AND AGRICULTURE APPLICATION

MD FAISAL KABIR

This thesis is approved as a creditable and independent investigation by a candidate for the Master of Science degree in Electrical Engineering and is acceptable for meeting the thesis requirements for this degree. Acceptance of this thesis does not imply that the conclusions reached by the candidate are necessarily the conclusions of the major department.

Qiquan Qiao, PhD — Date
Thesis Advisor

Steven Hietpas, PhD — Date
Head, Department of Electrical Engineering and Computer Science

Dean, Graduate School — Date

ACKNOWLEDGEMENTS

The research described in this thesis was supported by South Dakota State University Electrical Engineering Graduate Program and South Dakota Governor Research Center Program.

I would like to convey my sincere gratefulness to Dr. Qiquan Qiao for giving me a chance to work as a graduate assistant in his research group and for his enormous supports and guidance during the research period. Dr. Qiao's supports have been crucial in improving the quality of this thesis.

I would also like to thank Dr. Bjorn Vaagensmith, Mr. Ashim Gurung, Dr. Yung Huh, Dr. Parashu Kharel, and Dr. Charles Dieter for their time and consideration on reviewing my thesis. Moreover, I would like to thank my research group members for their support.

Finally, I would like to thank my family and friends for their love and support.

TABLE OF CONTENTS

LIST OF FIGURES

LIST OF TABLES

ABSTRACT

ELECTROCHEMICAL SENSOR FOR METAL IONS AND PHOSPHATE ION DETECTION FOR BIOMEDICAL AND AGRICULTURE APPLICATION

MD FAISAL KABIR

2017

The goal of this work was to develop electrochemical sensors for heavy metal ions (e.g., Cd^{2+}, Hg^{2+}, Pb^{2+}) and phosphate detections in fertilizers with high sensitivity, high detection range, repeatability and portability. The heavy metal electrochemical sensors were made using novel graphene oxide/silver nanowire (GO/AgNWs) composite as working electrode. The phosphate electrochemical sensors were fabricated using ammonium molybdate tetrahydrate/silver nanowires (AMT/AgNWs) modified screen printed electrode.

Most of the heavy metals such as mercury, lead, cadmium, and arsenic have dangerous effects on human body. These ions can enter human body system via agriculture food chain such as fish. Phosphorous-containing fertilizer is imperative to plant and animal nutrition. Essential biomolecules of the human body and plant growth depend upon the proper availability of phosphate ions in the fertilizer. There is a need for inexpensive, portable, repeatable, highly sensitive and field deployable sensors with high detection range to monitor the health of the field soil.

Mercury, lead and cadmium ions have oxidation peaks at three different potentials, which indicates good selectivity of the GO/AgNWs sensing electrode. In this experiment, the sensitivities of the GO/AgNW working electrode sensors are found to be 7.89 µA/µM,

4.21 µA/µM, 2.63 µA/µM for Cd^{2+}, Hg^{2+}, Pb^{2+} respectively. The detection ranges of these sensors are very broad at 5µM - 10 mM. From cyclic voltammetry measurements, the sensitivities of AMT modified SPE without and with AgNWs are 0.1 µA/µM and 0.71 µA/µM with a detection range of 5 µM - 50 mM. Therefore, the use of AgNWs increased the sensitivity of the AMT modified SPE significantly. I-V curves showed the sensitivities of the SPE without and with AgNWs are 0.2 Ω/µM and 1.6 Ω/µM, respectively. The sensors response shows a negative linear ($R \propto 1/Q$) relation between concentration (Q) and resistance (R). The repeatability tests show an error of only 5-6%. The sensing electrodes including GO/AgNWs composite film for heavy metal detection and AMT/AgNWs for phosphate ion detection invented in this work can be a potentially simple, low-cost system owing to easy fabrication processes and use of inexpensive materials; and portable as it is small and needs less equipment to collect data for field deployment.

Chapter 1: Introduction

1.1 Background

Heavy metals are considered as very toxic chemical elements. Additionally, they are characterized as metals because their atomic weights are near 63.5 and 200.6 $gmol^{-1}$and density larger than 5 gcm^{-3}. They are non-biodegradable, widely dispersed and present serious hazard to human health and environment. They are mixed in the earth and enter physical systems throughout the nutritious chain, causing weakening of human health. These metals make bonding with the thiol group of proteins and show their toxicity. Some metal ions are needed by the body system in a lower amount such as iron, cobalt, zinc, copper, manganese, and so forth, but higher concentration prompts to toxic impacts. However, heavy metals such as cadmium, lead, arsenic, chromium and mercury are deemed risky even at lower concentrations.

The above-mentioned ions are considered as the "Environmental health hazards" as they are positioned in the list of the 10 highest hazardous substances posted by Agency for Toxic Substances and Disease Registry (ATSDR**)**, based on the toxicity and potential contribution to polluted water, air and soil. A few international agencies such as World Health Organization (WHO), Center for Disease Control (CDC), Joint Food and Agricultural Organization (FAO), Joint FAO/WHO Expert Committee on Food Additives (JECFA), and International Agency for Research on Cancer (IARC) are working on the assessment of toxicity of these heavy metal ions. Among different important metals, lead (Pb), cadmium (Cd), mercury(Hg), arsenic (As) and chromium (Cr) are the most likely sources of metal ion-related sickness[1]. Small levels of metals are vital to the natural working of cells such as carrying cell signals. However, if the concentration exceeds the

limits, these metal ions can communicate with other standard protein leading to toxicity in humans, animals, and plants. The toxicity is caused by these toxic ions through enzyme inhibition, oxidative stress, and impaired antioxidant metabolism which can lead to unfavourable health impact. This can result in DNA harm, lipid peroxidation and reduction of protein sulfhydryl [2].

Phosphorous, nitrogen and water are the three main factors that determine the production of sufficient food to feed the fast-growing population of the world. Phosphorous-containing fertilizer is imperative to plant and animal nutrition[3]. Agriculture and agribusiness are one of the key industries in South Dakota. For example, 60% of South Dakota (USA) workforce directly or indirectly works in agriculture and over 43M acres are used as farmland. The agriculture commodities (e.g., corn, soybean, forage and wheat) and animal agriculture (e.g., cattle, turkeys and pigs) are valued at over $10B market. Annual fertilizer, chemical, seed costs are very high [4]. “Phosphate rock” provides around 80% of the world’s economically viable phosphorous. These rocks are localized in a single place and world’s supply of natural phosphorous is being threatened by worldwide political instability and monopolistic economic practices. Management of phosphorous is a bit inconsistent. Although the agriculture system may face the scarcity of phosphorous-containing fertilizer later this century, a lot of areas are now affected with an excess of phosphorous both inland and river water. Crops, livestock and energy production will need fresh water, which will considerably add to the existing pressure on non-renewable groundwater sources. It is anticipated that the scarcity of fresh water will be experienced by seven billion people in sixty countries by 2050. This will put further pressure both on food supplies and energy consumption rates [5]. In addition, food production creates huge

amount of waste streams that contain organic compounds, phosphorous- and nitrogen-containing species in water. Novel methods are needed to overcome the price of ineffective and energy intensive detection. The development of inexpensive, field-deployable, energetically and environmentally viable sensors to monitor phosphorous-containing species in agriculture and waste water would benefit the mass production of food and agricultural products.

Keup *et al.* reported that expanding the phosphate in a waterway led to the quick production of plankton, which made such water unacceptable for consumption [6]. The highest allowable concentration of phosphate in drinking water proposed by the World Health Organization is 1 mg L^{-1}. The determination of hyperparathyroidism, hypertension, vitamin D inadequacy, mineral, and bone tissue is related to phosphate condition in blood. The presence of phosphate amounts in body liquids can also give helpful data about infections, for example, kidney failure. The unusual level of phosphate in blood (hyperphosphatemia) can prompt to kidney harm. Bones and teeth get mechanical strength from phosphate salts. Body organs get phosphate from intestinal ingestion of food. Renal absorption and bone resorption are other important phosphate activities in our body [6]. Khoshiniat *et al*. found that phosphate detecting component might be available in different tissues and such sensor will distinguish changes in serum or nearby phosphate existence. Phosphate is a notable original part of cells which generates proteins in organic methods. The breaking of Adenosine triphosphate (ATP) in cells to produce energy greatly depends upon phosphate. Shervendani and Pourbeyaran observed a bone disorder due to phosphate related mineral. Polluted water treatment needs millions of dollars to expel phosphate from sewage before clearance. For these purposes, the censoring of phosphate fixation is vital

for improving water value and limiting contamination of regular waters. Quick, direct and delicate strategies for ensuring phosphate concentrations are key to empowering rapid evaluation of phosphate in different systems [7].

Compared to optical, electrical, electrochemical, mass and thermal sensors, electrochemical sensors are particularly preferable to detect metal and phosphate ions due to their exceptional selectivity, stability, and simplicity. A statistics of analytical chemistry improvement shows that electrochemical sensors are the quickly developing group of chemical sensors[7]. Preferably, a chemical sensor gives a particular reaction straight connected to a number of chemical compounds under investigation. All chemical sensors comprise of a transducer, which converts the obtained response into a recognizable data on prevailing equipment, and a chemically modified layer, which separates the signal of the chemical species from its surroundings. The chemical sensors can be classified according to the property to be detected as electrical, electrochemical, optical, mass or thermal sensors. These sensors are intended to identify and react to an analyte in the gaseous, liquid or solid state.

Electrochemical sensors have found meaningful employment in various applications such as clinical, mechanical, ecological and farming experiments. Potentiometric, amperometric and conductometric are three main parts of electrochemical sensors. Ion-selective electrodes (ISE), coated wire electrodes (CWES) and field effect transistors (FETS) are three major kinds of potentiometric devices. The ion selective electrode can detect particular ionic species. This system needs two electrodes which are working and reference electrodes. Voltage is applied externally to the working electrode. Reference electrode potential is determined by an electrolyte having the ion of interest.

Depending upon the type of the film, ISEs can be separated into three classes: glass, liquid and solid electrodes. ISEs are economically available more than twenty types from Orion, Radiometer, Corning, Beckman, Hitachi and others, and they are broadly utilized for the inspection of natural ions and of cationic or anionic ions in different solutions [8]. Freiser first presented coated wire electrodes (CWEs) in the mid of 1970's [9]. In the CWE method, an electrode is specifically coated with a proper polymer film generally poly (vinyl chloride), poly (vinylbenzyl chloride) or poly (acrylic corrosive) to make an electrode system that is sensitive to electrolyte fixations. The advantage of this sensor is that it does not require an internal reference electrode which leads simplicity in measurement. The FET is a solid–state tool that shows high-input impedance and low output impedance and is designed for observing charge development on the ion detecting film. The measurement depends on the equipment used to create microelectronic solid state chips [10], and its advantage is the feasibility to make tiny multisensory systems with various gates, for detecting several ions. In amperometric sensors, a voltage is applied to a reference and a working cathode to carry out the oxidation or reduction of chemical ions and the resultant current is calculated. In conductometric sensors, estimation of conductivity is done for a series of frequencies. Figure 1.1 shows various environmental applications of screen printed electrode (SPE) which is an electrochemical sensor.

Nowadays in electrochemistry, immobilization of chemical microstructures onto the surface of the electrode has become very common. Electrodes are modified chemically by use of a modifying mediator onto the electrode surface via chemical responses, chemisorption, composite formation or polymer coating. In contrast to normal working electrodes, this surface modification allows better control of working electrode features

and reactivity since the immobilization conveys the physiochemical properties of the mediator to the electrode surface [8].

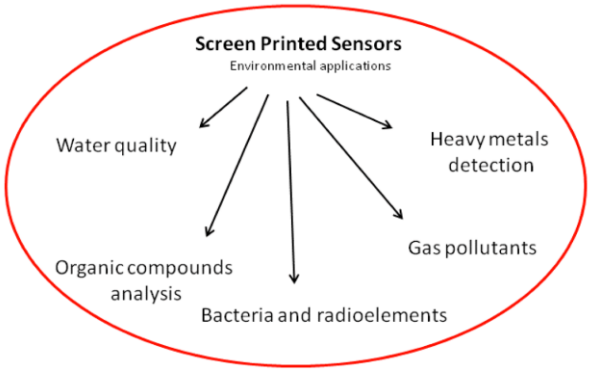

Figure 1. 1 Environmental application of electrochemical SPE [9].

This thesis is divided into two major parts: First part describes the graphene oxide (GO) /AgNWs electrode for sensing toxic heavy metal ions, and the second part illustrates SPE for phosphate measurement.

1.2 Literature review

For a long time, mercury was utilized as the most appropriate electrode material because of its exceptionally appealing qualities of regeneration, recodification and plane surface. These distinctive features of the mercury modified electrode prompted to the Nobel Prize in 1959 in Chemistry granted to Heyerovský. Both doping and hanging electrodes have been commonly utilized as a part of different polarographic and electrochemical techniques. With the advancement in electro-analytical science, different non-mercury electrodes have additionally been inspected. For instance, bismuth and carbon electrodes began to be utilized as a part of electro-investigation over three prior decades because of their minimal background current, suitable voltage range, ionic inertness and practicality for different sensing and detection purposes. They have disadvantages since

they use bulk pieces of metals which make the sensor design very enormous in size and not portable for field deployment. Nowadays, reduction in the size of solid electrodes has been used to achieve a decrease in sample volume, portability and cost effectiveness. Use of SPEs is one of the techniques to achieve the above-mentioned characteristics [11].

Graphene is a flat monolayer carbon. It has two-dimensional honeycomb-structured carbon atoms and has drawn a considerable attention because of its superior electronic, mechanical, optical and thermal features. It turned into a great candidate for a variety of applications such as transistors, transparent conducting electrodes, nanocomposites, lithium-ion batteries and gas sensors. Numerous techniques have been demonstrated for fabricating graphene layers including exfoliation, reduction of GO, chemical vapour deposition (CVD) and thermal desorption. Amongst them, reduction of GO is the mostly used method to fabricate the graphene layers with ease and for mass production. Oxygen functional groups such as hydroxyl, epoxide, carboxyl, carbonyl groups and defects can be used to modify the graphene layers. However, Hummers and modified Hummers techniques are the most widely used strategies to produce GO, which changes the physical and chemical characteristics of graphene [12].

Tang *et al.* reported aptamer-based GO/silver nanoparticles based electrochemical sensor to detect Pb^{2+} ions [13]. The detection range of this work was claimed to be in the range of 0.1 nM to 10 µM. They used aptamer which needs specific DNA sequence for the lead detection. This aptamer is very costly and is not abundant. Another group, Promphet *et al.* showed graphene/polyaniline/polystyrene nonporous fibers modified electrode to detect lead and cadmium simultaneously. The detection range for this device was 10- 500 μgL^{-1} [14]. The fabrication of the electrode with multiple layers is complicated.

Gnanaprakasam *et al.* demonstrated spongy spherical Au nanoparticles uniformly decorated on reduced graphene oxide (rGO) for simultaneous detection of Hg^{2+}, Pb^{2+}, Cd^{2+} ions. The Au nanoparticles showed good sensitivity of 19.05 mA mM^{-1}, 47.76 mA mM^{-1}, 22.10 mA mM^{-1} and 29.28 mA mM^{-1} for Cd^{2+}, Pb^{2+}, Cu^{2+} and Hg^{2+} [15]. Lately, Some *et al.* developed hydrophilic GO and hydrophobic rGO based fiber optic gas sensors to detect the unstable organic mixes such as CO_2, NO_3^-, etc. [16]. Recently, Cui *et al.* demonstrated the silver nanowires (AgNWs) modified GO composite sensors for the NH_3 vapor sensing. It was demonstrated that the sensitivity of GO-Ag nanolayer was higher than that of GO and multi-walled carbon nanotubes-Ag nanocomposites as Ag nanoparticle has good enhancing capability, conductivity and stability [17]. Moreover, the loading thickness of AgNWs significantly influenced the sensing performance of GO-AgNWs hybrid, and an appropriate nanoparticle loading led to higher sensitivity. However, the fabrication procedures of the above sensors are complicated and costly. Noble metal nanoparticles such as Ag, Au, Pt, and Pd were used to make GO-metal nanoparticle mixtures [15]. The existence of metal nanoparticles on GO surface greatly enhanced the capacity of ammonia gas sensing due to their improved surface to volume proportion. The presence of different oxygen functional groups such as hydroxyl, epoxide, carbonyl and carboxyl groups in GO allowed AgNWs to interrelate with the GO layers with electrostatic binding or charge-transmission interface. The presence of AgNWs on the GO surface can potentially enhance the detection function toward ions over partly reduced GO sensor [12]. Carbon or polymer-based materials have moderately small electrical conductivity and sheet resistance higher than that of ITO/glass. Percolation junctions of AgNWs have demonstrated comparable sheet resistance and transparency of ITO/glass. Due to the high

conductivity of silver, the sheet resistance of an AgNWs permeation junction is determined by the interaction resistance of inter-nanowire networks [18].

Many works have been reported for the detection of phosphate. A system based on spectrophotometric determination was among the first analytical devices developed. These colorimetric methodologies are typically based on the phosphomolybdate blue complex and characterized by the turbidity. These strategies are influenced by silicate obstruction; the silico-molybdate blue complex has a wide absorbance band (790 nm) that covers 710 nm commonly utilized for phosphomolybdate blue sensing. Rohwedder *et al.* demonstrated a mono segmented drift system for the detection of phosphate in water, by utilizing the response between molybdophosphate and malachite green, characterized by high absorption at 650 nm. However, the colorimetric setup is difficult to adjust for online estimations, since it requires plenty of reagents and is ascorbic corrosive. The advantage of the electroanalytical procedure is that it does not require ascorbic acid because the reduction occurs at the electrode surface. Moreover, they are characterized by cost-effective equipment and suitable to be used directly in-situ by means of portable equipment interfaced with a portable computer. Talarico *et al.* reported the use of SPE modified with carbon black to detect phosphate ions and their limit of detection was 6 µM [19]. The sensitivity here was not linear, and the carbon black is not a good conductive material. Gilbert *et al.* used pyruvate oxidase to make the electrochemical sensor where the pyruvate oxidase reacts with the phosphate ions and produce hydroxide ions giving the chemical response. The detection limit was 23 µM to 180 µM [20]. The main limitation of the reported electrochemical sensors is lower sensitivity. They used the bulky instrument to get the data which make them non-portable and non-field deployable.

In summary, various approaches such as modified carbon and graphene based electrodes were made previously, but they are not portable, field deployable, very expensive and complicated to make. In addition, bulky instruments are needed to obtain data.

1.3 Motivation

There is a need for low cost, portable, repeatable, highly sensitive and field deployable sensors with wide detection range to monitor the agriculture field soil and biomedical applications.

1.4 Objectives

The goal of this work was to develop simple electrochemical sensors using novel GO/AgNWs for heavy metal ions detection and novel modified SPE for phosphate detection to achieve simplicity, high sensitivity, wide detection range, repeatability and portability. The tasks to achieve the goal were to:

1. Prepare precursor solutions including preparation of AgNWs, GO/AgNWs mixtures, an electrolyte for metal and phosphate ions, ammonium molybdate tetrahydrate, different concentrations of metal and phosphate ions.
2. Clean samples and conduct plasma treatment.
3. Fabricate electrochemical sensor devices including sensor electrode, AgNWs and Phenyl-C61-butyric acid methyl ester (PCBM) on working electrode of SPE.

4. Characterize the sensors with Raman spectroscopy, scanning electron microscopy, cyclic voltammetry and Agilent 4155C semiconductor parameter analyzer.

1.4 Organization of dissertation

Chapter 1 describes the need for electrochemical sensor devices, classification of electrochemical sensors, need of heavy metal ion and phosphate ion detection in ground water and complexity in developing different kinds of sensor devices. Finally, motivation, goal, and specific tasks of this work are presented.

Chapter 2 discusses the basic working principle of electrochemical sensors. The sensors have different parameters that affect the sensor performance. The theory behind the parameters and characterization techniques are described.

Chapter 3 describes experimental details of preparing GO/AgNWs films and ammonium molybdate tetrahydrate/AgNWs modified SPEs. The characterization techniques used for analysis of sensor device performance are described.

Chapter 4 presents the results of the sensor device performance using different characterization techniques to demonstrate the sensor selectivity and sensitivity. The difference between the sensor performance of with and without AgNWs are discussed in this chapter.

Chapter 5 summarizes this work with key conclusions and future work.

Chapter 2: Theory

2.1 Working principle of an electrochemical cell

Electrochemistry defines the relationship between chemical reactions and energy or power associated with it. This involves the investigation of compound conversions produced by the passing of an electric current over a system, or the generation of electric power by chemical reactions.

Numerous chemical reactions require input energy to occur. Such reactions typically take place at the surfaces of cathodes in an electrochemical cell. These reactions provide data about the types and characteristics of the chemical ions held in the cells. The generation of chlorine and aluminium, electroplating and electrowinning of metals are examples of modern electrochemical procedures. Electrochemical cells that create electric energy from chemical reaction are the foundation of main and auxiliary energy cells [21].

Current and potential (or voltage) are the subjects of interest for electrochemical cells. Current is measured in ampere (A) which is the measure of charge in coulombs (C) that goes over a medium per second. Voltage among the two electrodes is computed in volts (V) with a voltmeter and is the measure of the energy of the cell response. Measurements of the voltages of galvanic cells at open circuit provide information about the thermodynamics of cells and cell responses. For instance, the voltage of the galvanic cell shown in figure 2.1 is 1.10 V when the mix concentration is 1 molar (1 M) at 25°C, this is known as the standard potential of the cell and is denoted by E°. The obtainable energy (Gibb's free energy $\Delta G°$) of the cell response is identified with E° by the equation:

$$\Delta G° = -nFE° \quad \text{.....2.1}$$

where n is a number of electrons involved in the reaction and F is the Faraday's constant (96,485 coulombs/mol). The cell potential is the difference in potential of the two half-cells. The half-cell reaction $Cu^{2+} + 2\ e^{-} \rightarrow Cu$ has standard potential of $E° = +0.34$ V versus NHE (Normal Hydrogen Electrode) and correspondingly, the standard potential for the Zn/Zn^{2+} cell gives $Zn \rightarrow Zn^{2+} + 2\ e^{-}$ is -0.76 V. The reaction of copper is called reduction and the reaction of zinc is called oxidation. These two reactions must take place at the same time to successfully operate the electrochemical cell.

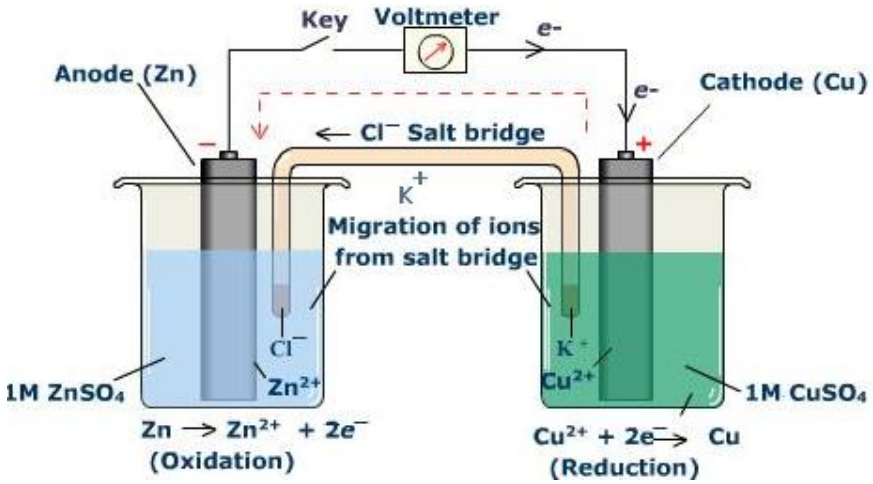

Figure 2. 1 Galvanic cell showing oxidation and reduction reactions[22].

Voltammetry belongs to a categorization of electro-analytical techniques, through which information about an analyte is collected by varying a voltage and calculating the resultant current. It is, therefore, an amperometric procedure. Since there are various approaches of varying the voltage, there are in addition many forms of voltammetry, for example, polarography (DC Voltage), linear sweep, differential staircase, normal pulse, reverse pulse, differential pulse and others. Cyclic voltammetry is one of the greatest commonly used techniques and provides data about the redox potential and electrochemical response rates of ionic mixtures. In this case, the potential is swept from V1 to V2 at a

constant rate, and when the voltage achieves V2, the sweep is opposite, and the potential is swept back to V1, as is represented in Figure 2.2(a). The scan rate, (V2 - V1)/ (t2 - t1), is a crucial thing since the length of a sweep must give enough time for a significant chemical response to happen. Changing the scan rate, therefore, gives respectively varied results. Potential is applied between the reference electrode and the working electrode, but the current is acquired among the working and the counter electrodes.

The acquired measurements are plotted in a graph as current versus voltage, also known as voltammogram as shown in a typical example in figure 2.2(b). As the voltage is enhanced towards the electrochemical reduction voltage of the ions, the current will also increase. When the voltage of V2 increases, and exceeds this reduction potential then the current starts to decrease. As the voltage is switched towards V1, the reaction will start to reduce the product from the initial reaction. This creates an increase in current of opposite polarity as compared to the forward sweep, but again decreases below the reduction potential. The reverse scan also gives data about the reversibility of a reaction at a given sweep rate. The form of the voltammogram for a specific analyte depends on several factors such as electrode surface characteristics, scan rate, catalyst type and concentration.

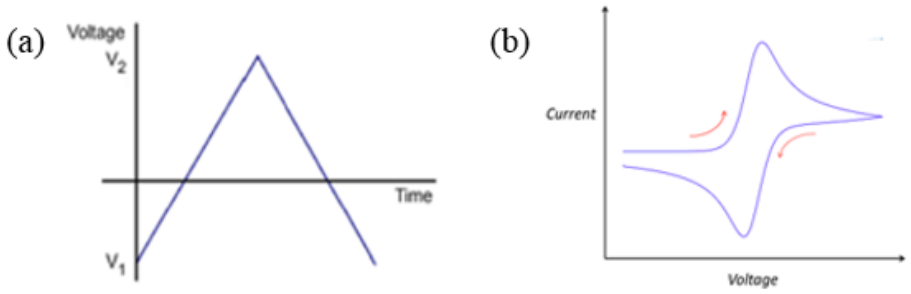

Figure 2. 2 An example of cyclic voltammograms: (a) a single generic linear voltage scan and (b) a cyclic voltammogram of the Prussian Blue-changed (PB) glassy carbon electrode set up in 0.1 M KCl + 0.1 M HCl with a scan rate 50 mV/s [23].

2.2 Working principle of electrochemical sensing electrodes

2.2.1 Graphene oxide (GO)

GO is a single layer of carbon atoms in which the atoms are firmly packed in a honeycomb-like crystal lattice as shown in figure 2.3. The properties of GO including large surface area, low production cost and catalytic properties and so forth make it a potential material in the field of sensing. The existence of various oxygen functional groups which covalently attached to carbon atoms making GO hydrophilic. It has a high Young's modulus (~0.25 TPa) and high flexibility, making it a greatly rigid component. In addition, GO is cheap and solution processable.

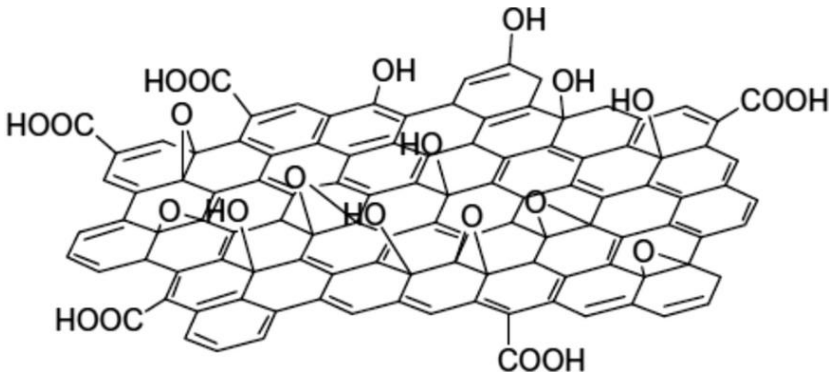

Figure 2. 3 Chemical structure of GO [21].

2.2.2 Role of AgNWs in sensing

AgNWs can be involved by epoxy, carboxyl, hydroxyl, and carbonyl functional groups and adsorbed on the top of GO via Ag–π orbital connection as shown in figure 2.4. These functional groups give improved electrostatic interface among Ag-GO and negatively charged GO and form an Ag–GO composite. Having oxygen functional groups, metal molecules that are considered as an electron donor can be adsorbed on the plane of GO-AgNWs layer, providing a good detection ability. Figure 2.4 shows the working

mechanism of GO-AgNWs film. It can be seen that metal ions can be attached to the surface of the working film.

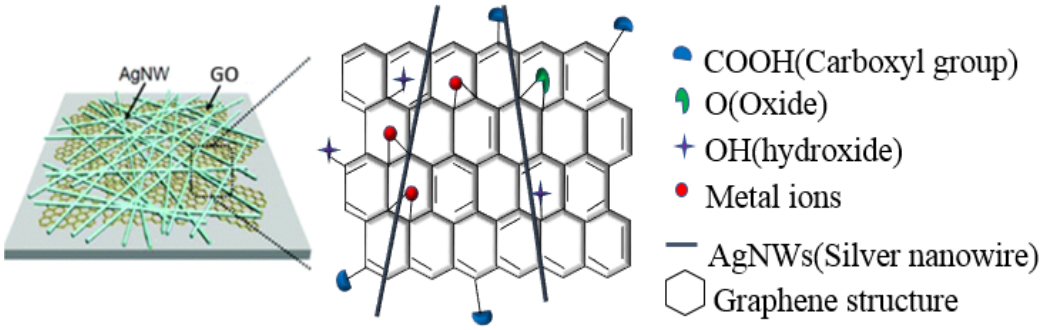

Figure 2. 4 Mixture of GO-AgNWs showing the attachment of metal ions.

2.2.3 Mechanism of SPE

SPEs are industrially made for electrochemical reaction to use in environmentally friendly biomedical and agriculture areas. They are typically made of carbon, gold, platinum, silver, carbon nanotubes. The general strip dimension is 3.4 x 1.0 x 0.05 cm. This device is very inexpensive and reusable for microvolumes of samples. The working electrode of the screen-printed electrode is modified with AgNWs and ammonium molybdate tetrahydrate. The oxidation reaction occurs in two steps. It is known that in a compound when oxygen is added then the reaction is oxidation. Here in this reaction, the $Mo_7O_{24}^{6-}$ and H^+ are oxidized in two different steps as shown in the reaction 2.2a. 2.2b shows the reduction reaction of the working electrode. That is why two oxidation peaks were found, and again the phosphate has changed its valence from 5 to 7. The reaction of the working electrode with phosphate ions takes place as:

$$7H_3PO_4 + 12Mo_7O_{24}^{6-} + 51H^+ = 7PMo_{12}O_{40}^{3-} + 36H_2O \quad \text{..... (2.2a)}$$

$$PMo_{12}O_{40}^{3-} + nH^+ + ne^- = [H_n\, PMo_{12}O_{40}]^{3-} \text{.....(2.2b)}$$

The peak current depends on the change of concentration via the following equation:

$$i_P = (2.69\times10^5)n^{3/2}AD_0^{1/2}V^{1/2}C_0^* \text{ [24]} \quad \text{..... (2.3)}$$

Where, i_P = peak current, n = the number electron, A = area of the working electrode (cm^2), D_0 = diffusion coefficient (cm^2/s), V = scan rate (V/s), C_0^* = concentration of the oxidized materials in solution. As n, A, D_0, V are constant. Thus, it can be simplified as,

$$i_P \propto C_0^* \quad \text{..... (2.4)}$$

The peak current varies proportionally with concentration. The current vs concentration plot of cyclicvoltammetry measurement should be linear.

For the I-V measurement, the current varies with charge concentration. Faraday's first law of electrolysis shows,

$$I = \frac{Q}{t} \quad \text{..... (2.5)}$$

Where, I = current (A), Q= charge (coulomb) and t= time (s)

From Ohm's law,

$$I = \frac{V}{R} \quad \text{..... (2.6)}$$

Where, V= applied voltage (V) and R= resistance (Ω)

As V and t are constant, so from equation 2.5 and 2.6 it is found that,

$$R \propto \frac{1}{Q} \quad \text{..... (2.7)}$$

Which depicts a negative linear relationship between resistance and charge concentration

2.3 Working principle of characterization techniques

2.3.1 Raman spectroscopy

Raman spectroscopy can provide a fingerprint of a molecule with which a particular ion can be determined. The peak position and intensity can give the information about the concentration of specific ions. So, it is important to detect ions. Figure 2.5 describes the schematic diagram of light scattering after laser falls on a sample plane. When monochromatic radiation falls upon a sample, it can be reflected, absorbed or scattered. It is the scattering of the radiation from the sample that provides information about the atomic structure of the sample. The photons are scattered by the sample, so their wavelengths are also changed which provides the chemical and structural data. The scattered radiation consists of both incident radiation wavelength (Rayleigh scattering) and a little measure of radiation that is scattered with another distinct wavelength (Stokes and Anti-Stokes Raman scattering) (approx. just 1 x 10^{-7} of the scattered light is Raman). Light scattered from a particle has a few elements - the Rayleigh scattering, and the Stokes and Anti-Stokes Raman scatter. In atomic structures, these frequencies are primarily of the kinds related with rotational, vibrational and electronic level transitions. The scattered radiation happens over all ways and may also have changes in its polarity alongside its wavelength. The scattering procedure without a variation of frequency is called Rayleigh scattering and is a similar procedure demonstrated by Lord Rayleigh and which represents the blue color of the sky. So, Raman scattering is called a variation in the frequency. Raman moved photons of light which can be both of higher or smaller energy, dependent on the vibrational condition of the atom [25].

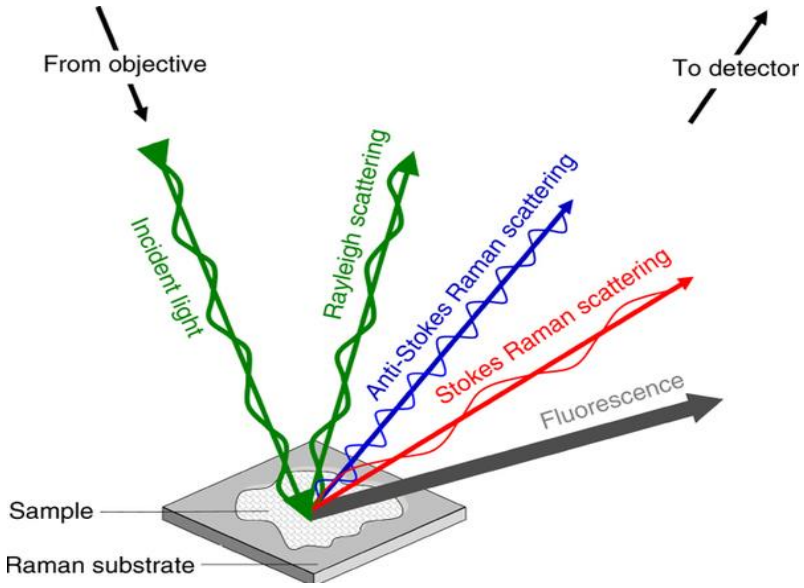

Figure 2. 5 Schematic showing light scattering after laser falls on a sample plane [26].

2.2.1 Scanning electron microscope (SEM)

SEM characterization of the sensor electrodes was carried out to observe the film quality and morphology of the electrode surface. Figure 2.6 describes the schematic diagram of SEM working principle. The scanning electron microscope (SEM) uses a concentrated emission of high energy electrons upon a sample. The signals that get from electron-specimen contacts provide data about the sample in addition to outside morphology (texture), chemical mixtures, and crystalline structure and polarization of components which are inside the sample. The SEM is additionally equipped with for investigating of specified areas on the sample; this method is particularly helpful in deciding chemical compositions (utilizing EDS), crystalline structure, and crystal orientations (utilizing EBSD)[27].

The electrons which get accelerated in a SEM provides the data of kinetic energy, and this energy is dissolved as different signals delivered by electron-sample connections

when the solid sample decelerate the incident electrons. These signals comprise secondary electrons (that deliver SEM images), backscattered electrons (BSE), diffracted backscattered electrons (EBSD that are utilized to decide crystal arrangements and orientations of atoms), photons (typical X-rays which are used for basic investigation), visible light (cathodoluminescence–CL), and heat. Secondary electrons are utmost important for demonstrating morphology and topography on surfaces, and backscattered electrons are very important for illustrating contrasts in the composition in multiphase specimens (i.e. for fast phase separation). X-ray generation is delivered by rigid collisions of the occurrence electrons with electrons in discrete orbitals (shells) of particles in the sample. As the energized electrons come back to lower energy states, they give X-rays that are of a constant wavelength (that is identified with the difference in energy levels of electrons in various shells of a component). Along these lines, characteristic X-rays are generated for every component in a mineral that is "energized" by the electron beam.

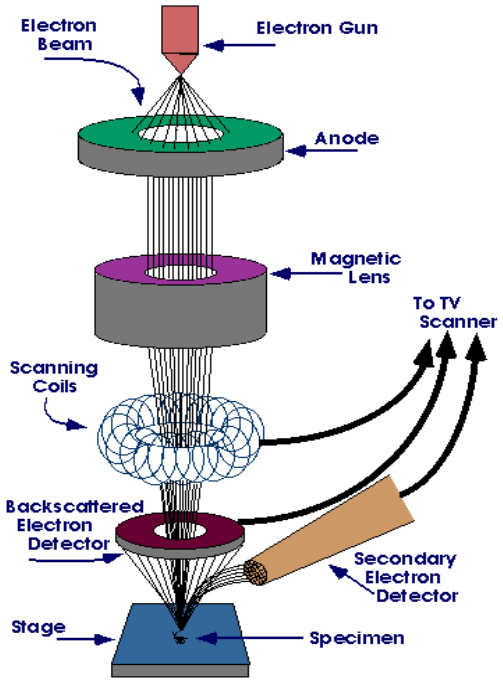

Figure 2. 6 Set up of Scanning Electron Microscope [28].

Chapter 3: Experimental procedures

3.1 Preparation of precursor solutions

3.1.1 Fabrication of AgNWs solution

Figure 3.1 shows the preparation of AgNWs. Silver nitrate was purchased from Sigma Aldrich. Two knob flask was taken and cleaned with soap and deionized (DI) water. The stirrer was put inside the biker and was sonicated with soap water, DI water, acetone and IPA for 20 minutes for each. 6 ml of ethylene glycol (EG) and 0.5 g of silver nitrate ($AgNO_3$) were mixed in a cylinder. 0.025M $CuCl_2$ solution was prepared in EG. A big pyrex biker was taken to use oil and an RTD thermometer to measure the temperature. 0.3g polyvinylpyrrolidone (PVP) was added slowly in 24 ml of EG with the moving stirrer in a flask and was heated in the oil bath at 150˚C, but the RTD showed 175˚C When the temperature was stable then, 40 µL of $CuCl_2$ was added, and stirred 1 minute at 260 rpm at the same temperature.

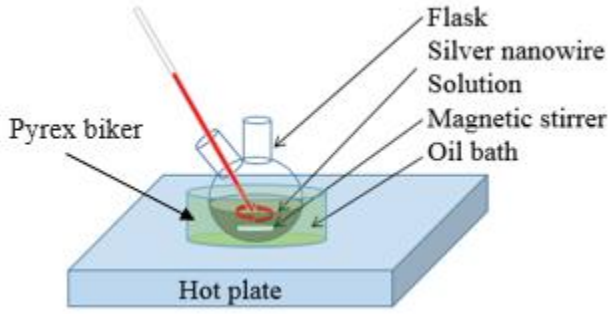

Figure 3. 1 Set up to prepare AgNWs.

The $AgNO_3$/EG solution was sonicated for 4 minutes until it turned little yellow before adding to the biker. $AgNO_3$/EG solution was added slowly to the biker which took almost 10-15 minutes. Longer heating time might make the nanowires thicker. High

temperature might make the reaction faster. 0.9 g to 0.3 g of PVP was added to test the effect of concentration of PVP on nanowires morphology. The centrifuging was done four times to clean the uncleaned AgNWs, first with acetone, followed by DI water for the remaining three times. Each time the centrifuging was done for 20 minutes at 2000 rpm. After that IPA was used to preserve the AgNWs. Each time the nanowires were shaken and mixed with the cleaning solution before centrifuging.

3.1.2 Preparation of GO/ AgNWs solution

Aqueous GO solution was purchased from Sigma-Aldrich which has a concentration of 4 mg/ml. The AgNWs were centrifuged for 5 minutes at 1000 rpm. The wires were diluted in IPA to achieve 4 mg/ml. Then the nanowires were centrifuged and dispersed in GO solution.

3.1.3 Preparation of electrolyte solution for metal ions

The electrolyte was an essential solution consisting of 5 mM of potassium ferrocyanide ($K_4FeCN_{6)}$ and 0.1 M of potassium chloride (KCl) and had a volume ratio of 1:1. 0.05 ml of 10% w/w solution of K_4FeCN_6 was taken to make 5 ml of the solution, and 0.04 g of KCl was mixed with 5 ml of water to make 0.1 M KCl solution.

3.1.4 Preparation of ammonium molybdate tetrahydrate (AMT)

100 g of ammonium molybdate tetrahydrate was purchased from Sigma-Aldrich. 0.013 g of AMT was dissolved in 10 ml of DI water to prepare 10 ml of solution. This solution was used to find out the oxidation peaks for phosphate detection.

3.1.5 Preparation of electrolyte solution for phosphate detection

98% sulfuric acid was purchased from Fisher Scientific. A stock solution of sulfuric acid was calculated as 18.385 M based on a density of 1.84 g/mL, a molecular weight

of 98.08 g/mol, and a concentration of 98% w/w. To make a 0.1 M solution, 0.054 mL of stock solution was added slowly to 2.5 mL deionized water. The final volume of solution was adjusted to 10 mL with deionized water.

3.1.6 Preparation of metal ion solution with different concentration

Mercury chloride ($HgCl_2$), cadmium nitrate($Cd(NO_3)_2$) and lead iodide(PbI_2) were bought from Sigma-Aldrich. Then the weight was calculated to make different molarity solution. The mass (m) of the metal ion precursor was calculated from the equation:

$$m = c \times v \times mw \quad \ldots\ldots\ldots\ldots\ldots\ldots\ldots\ldots\ldots\ldots\ldots\ldots\ldots\ldots \quad (3.1)$$

where c is molar concentration (mol/L), v is the volume (L), and mw is the molecular weight (g/mol).

Firstly, 1 M of $HgCl_2$ was made by adding 1.36 g of $HgCl_2$ powder in 5ml of water. From this 1 M solution, 10 µM, 50 µM, 100 µM, 200 µM $HgCl_2$ solutions were obtained by adding 0.05 µl, 0.25 µl, 0.5 µl and 1 µl in 5 ml of DI water respectively. Secondly, 1 M of PbI_2 was made by adding 4.6 g of PbI_2 powder in 5ml of water. From this 1 M solution, 10 µM, 50 µM, 100 µM, 200 µM PbI_2 solutions were made by adding 0.05 µl, 0.25 µl, 0.5 µl and 1 µl in 5ml of DI water respectively and thirdly, 1 M of $Cd(NO_3)_2$ was made by adding 1.18 g of $Cd(NO_3)_2$ powder in 5 ml of water. From this 1M solution, 10 µM, 50 µM, 100 µM, 200 µM $Cd(NO_3)_2$ solutions were made by adding 0.05 µl, 0.25 µl, 0.5 µl and 1 µl in 5 ml of DI water respectively. Different concentrations of $HgCl_2$, PbI_2, $CdNO_3$ solutions were dropped on the film and waited 5 minutes to become dry before the measurement.

3.1.7 Preparation of phosphate ion solution with different concentrations

Sodium biphosphate(Na_2HPO_4) was purchased from Sigma-Aldrich. It has a molar

mass of 141.16 g/mol. So, 0.7 g of it was taken and mixed with 5 ml of DI water. Then, from this 1M solution, 10 µM, 50 µM, 100 µM, 250 µM, 500 µM, 750 µM, 1 mM PbI_2 solutions were made by adding 0.05 µl, 0.25 µl, 0.5 µl, 1.25 µl, 2.5 µl, 3.75 µl and 5 µl in 5 ml of DI water respectively.

3.2 Sample cleaning and plasma treatment

Fluorine doped Tin Oxide (FTO) substrates were sonicated with soap water, DI water, Acetone and IPA for 20 minutes for each. Then they were dried with dry nitrogen(N_2) gas and were placed inside the plasma cleaner as shown in figure 3.2. The purpose of cleaning the sample and doing the plasma treatment was to make the surface hydrophilic that leads to better adhesion. The chamber was evacuated using a mechanical pump. FTO substrates were kept under vacuum for 5 minutes. An oxygen cylinder knob was then opened which was previously connected to the plasma cleaner at ~50 psi for 1 minute. The RF power level was set to medium. The oxygen valve was turned on for 10 seconds after every 5 minutes of interval. This process continued for 20 minutes. After that, the power was turned off as well as the oxygen knob and the air knob was turned on slowly. Finally, the oxidized samples were taken out from the plasma cleaner.

Figure 3. 2 Picture of oxygen plasma cleaner.

3.3 Electrochemical sensor device fabrication

3.3.1 Fabrication of sensor electrode

Two types of electrodes were prepared namely, composite (Figure 3.3) and layer by layer (Figure 3.4). For the composite electrode, the GO/AgNWs mixture solution was spin coated at 2000 rpm on a cleaned FTO glass substrate with an acceleration of 2000 rpm for 30 seconds. For layer by layer electrode, firstly GO was spin coated on the cleaned FTO glass followed by drop casting of the AgNWs solution on top of the GO film and drying for 30 minutes in the air. Different concentration of metal ions solutions was dropped and waited 5 minutes and then tested.

Figure 3. 3 Composite electrodes of GO/AgNWs.

Figure 3. 4 Layer by layer electrode of GO/AgNWs.

3.3.2 Fabrication of AgNWs on working electrode of SPE

SPEs were purchased from DropSens. The working electrode was made of carbon which was modified with AgNWs and AMT as shown in figure 3.5. The modification was done by dropping the prepared solutions of AgNWs and AMT over the carbon working electrode and making it dry in air for 30 minutes. Different concentration of phosphate ion

solutions was dropped and waited 5 minutes and then tested. The measurements were carried out with and without the AgNWs.

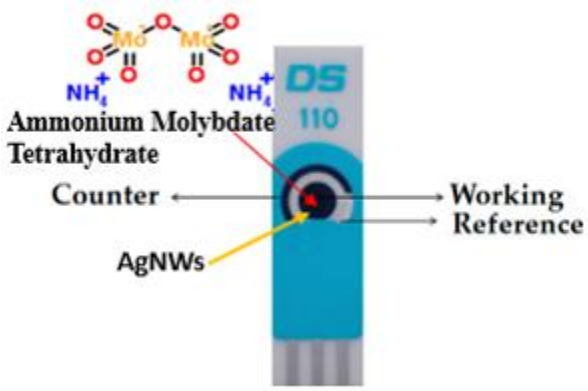

Figure 3. 5 Image of the modified SPE.

3.3.3 Modification of working electrode of SPE with Phenyl-C61 butyric acid methyl ester(PCBM)

The carbon working electrode was modified with PCBM, and the other area was etched with chlorobenzene. The electrolysis process was carried out between the electrodes applying 10V DC voltage across the working electrode and counter electrode. The PCBM had been used due to its better electron accepting ability and relatively high electron mobility.

3.4 Characterization of the sensor electrodes

3.4.1 Scanning electron microscopy (SEM)

SEM characterization of the sensor electrodes was carried out to observe the film quality and morphology of the electrode surface. The Hitachi S-4300N as shown in figure 3.7 was used to obtain the SEM images. The machine and the software for SEM were turned on with a small key and in computer respectively. The sample chamber was opened

manually after filling with air. GO/AgNWs films with different structures and compositions were placed in the chamber and EVAC icon in the software was pressed to make the chamber vacuum. The sample holder was automatically adjusted near the detector. Each time 25kV was applied, and the current started to increase. There were a monitor and focusing knobs on doing the zooming perfectly. Different range of zooming images was selected to get the images of the film surface.

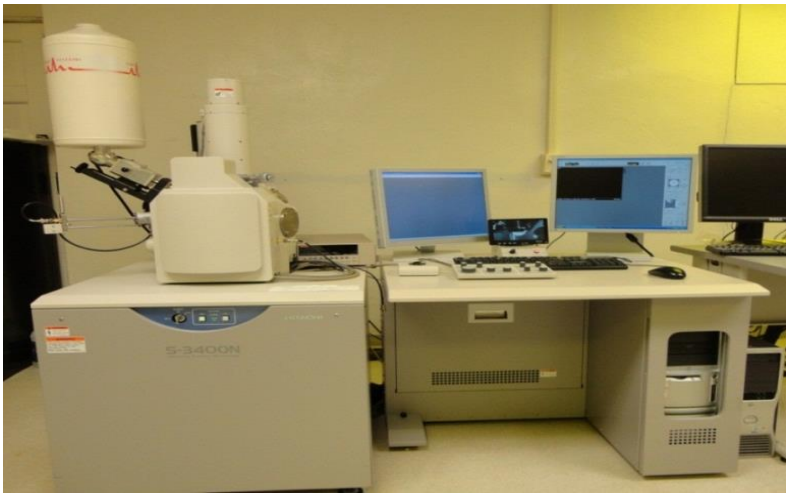

Figure 3. 6 Photograph of Hitachi S-4300N SEM.

3.4.2 Raman spectroscopy

Raman measurements of different GO/AgNWs films was carried out to determine the signature peaks of the metal ions under investigation. This was done by using the LabRAM HR Evolution system as shown in figure 3.6. Labspec5 software was opened on the computer which controls the Raman spectroscopy. Different structures of GO/AgNWs films with different concentrations of metal ions were placed on the stage, and x100 magnifying lens was focused on the sample. The green laser which has a wavelength of 532 nm was used for the experiment. Diffraction grating and filter intensity were set at

1800 and D2 respectively. The video camera was turned on which was also connected with a light source through an optical fiber. To adjust the sample stage, a joystick was used. After the adjusted zooming, the spectrum acquisition icon was selected in the software to get the final spectrum.

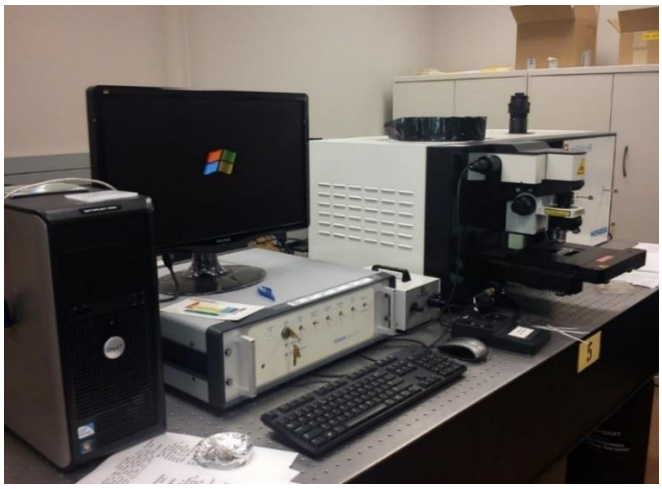

Figure 3. 7 Photograph of the LabRAM HR Raman spectroscopy.

3.4.3 Cyclic voltammetry (CV)

CV measurements were done using a computer connected Ametek VERSASTAT3-200 potentiostat as shown in figure 3.8. The cyclic voltammetry (single) measurement was chosen. The initial, vertex and final potentials were selected as -1V, 1V and -1V respectively. The scan rate was selected as 50 mVs^{-1}. After extracting data from cyclic voltammetry measurements, potential vs. current was plotted using the versastudio software. The electrolyte was 1:1 volume mixture of 5 mM $K_4Fe(CN)_6$ and 0.1 M KCl in water. The set up included GO/AgNWs as working electrode, Ag/AgCl as a reference electrode and platinum as the counter electrode. For phosphate ion detection, AMT/AgNWs modified carbon, carbon and silver were the working, reference and counter electrode respectively.

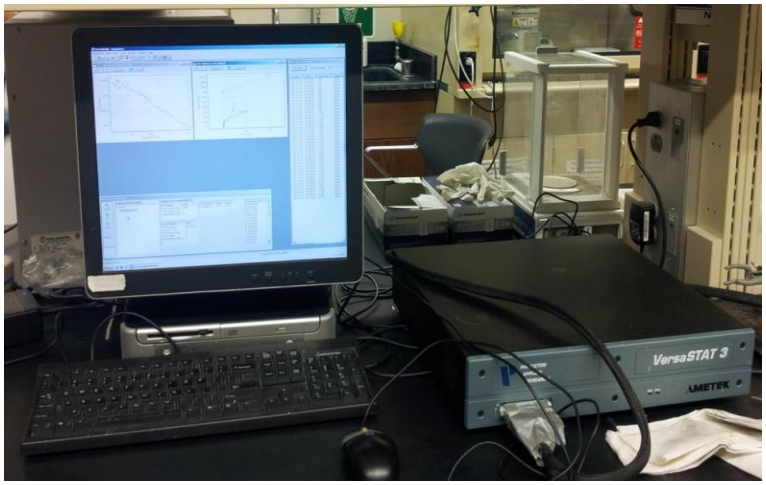

Figure 3. 8 Photograph of VERSASTAT3-200 potentiostat electrochemical cyclic voltammetry.

3.4.4 Current-voltage (I-V) characterization

Figures 3.9 shows a photograph of Agilent 4155C semiconductor parameter analyzer used for extracting I-V data of sensor devices. The test voltage ranges were 0 to 3V for all the screen-printed electrodes.

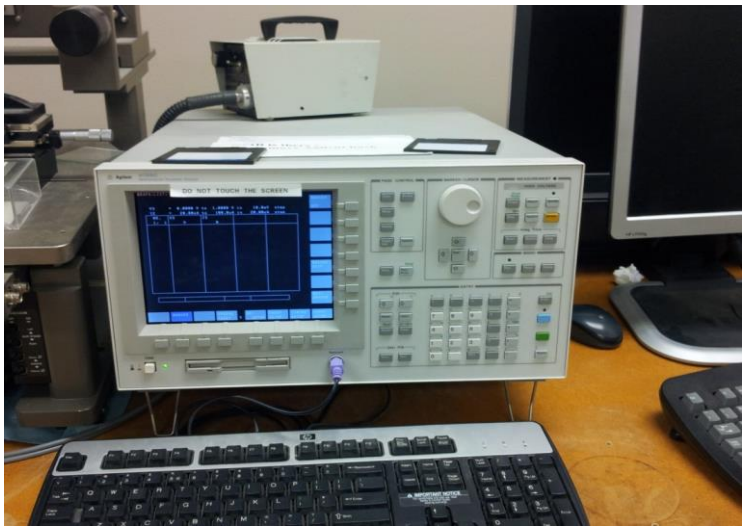

Figure 3. 9 Photograph of Agilent 4155C semiconductor parameter analyzer to extract I-V data of sensors.

Chapter 4: Results and analysis

4.1 Morphology of growth of AgNWs on top of GO layer

Figure 4.1a shows the microscopic images of GO/AgNWs composite layer where the dark area is GO, the bright lines are AgNWs, and the light area is FTO substrate. Figure 4.1b shows the SEM image of GO/AgNWs layer. It can be seen that the AgNWs are well spread over the entire surface of the GO.

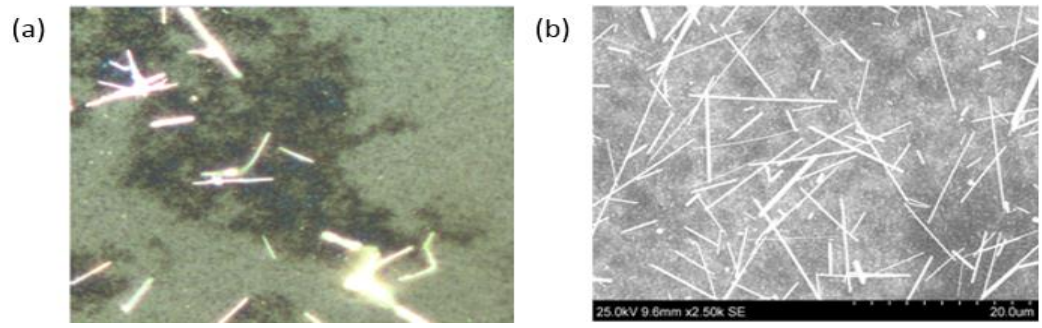

Figure 4. 1 (a) Microscopic image of GO/AgNWs composite layer. (b) SEM image of GO/AgNWs layer.

Figure 4.2 shows the SEM images of AgNWs synthesized with heating for a reaction time of (a) 10 min and (b) 16 min. Here, it can be seen that the shorter reaction time yielded longer AgNWs with an average value of 29 μm for 10 min compared to the 15 μm for 16 min.

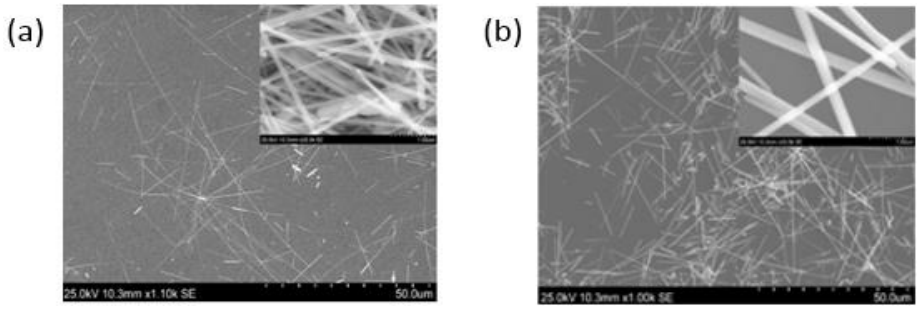

Figure 4. 2 SEM images of AgNWs from reaction time of (a) 10 min and (b) 16 min heating.

In addition, the AgNWs were thinner with a diameter of around 100 nm for shorter reaction time at 10 min, whereas the diameter increased to 125 nm for longer reaction time at 15 min. However, some agglomerates were observed on the film for longer time at 16 min.

4.2 Raman spectrum change for the detection of metal ions with GO/AgNWs films

4.2.1 Raman spectroscopy for GO/AgNWs films

Figure 4.3 shows Raman spectra for GO only, GO/AgNWs mixed composite and GO/AgNWs layer by layer structure. Raman shifts at 1300 cm^{-1} and 1500 cm^{-1} which represent the characteristic peaks for GO. The intensities of the Raman peaks were different in the GO/AgNWs composite and layer by layer structures of sensors. The Raman peak intensity in the layer by layer structure was higher than the mixed structure. The layer by layer structure was chosen for the experiment as it was more sensitive. The incorporation of AgNWs increased the intensity of the Raman peaks.

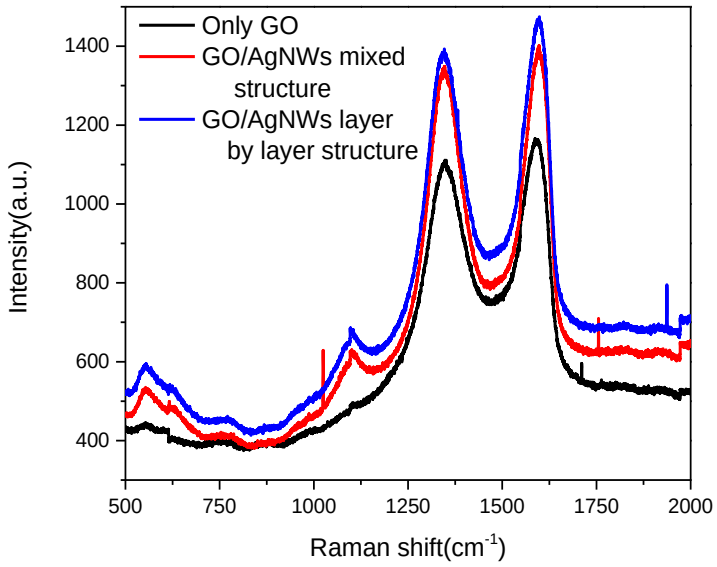

Figure 4. 3 Raman spectra for GO only, GO/AgNWs composite and GO/AgNWs layer by layer structure.

4.2.2 Raman spectra for mercury chloride ($HgCl_2$) to detect mercury

Figure 4.4 shows the Raman spectra of the sensing electrode in response to the different concentration of mercury ions. It can be observed that the peak intensity decreased with the decrease of concentration of $HgCl_2$. This indicated the concentration sensitivity of the film . The peak varied at around 230 cm^{-1}. The intensity varied from 200 to 8000 for 10 µM to 1 mM of mercury ions. More mercury ions are attached on the film surface with the increase of concentration, resulting in higher peak intensity. Also, it is selective as it showed peaks only at 230 cm^{-1} which indicated the presence of mercury.

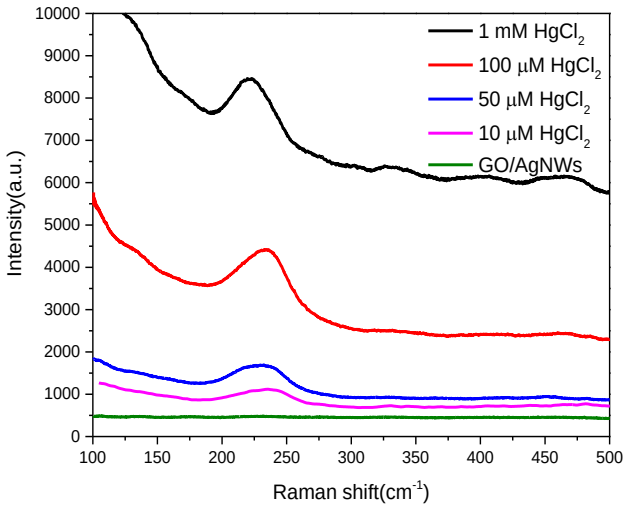

Figure 4. 4 Raman spectra of the GO/AgNWs electrode in response to different concentrations of mercury ions: 10 µM, 50 µM, 100 µM and 1 mM.

4.2.3 Raman spectra for cadmium nitrate to detect cadmium ions

Figure 4.5 shows the Raman spectra of the GO/AgNWs electrode in response to different concentrations of cadmium ions. The intensity of the Raman peaks at 1350 cm^{-1} and 1600 cm^{-1} changed with the change in cadmium concentrations. For 10 µM, 50 µM, 100 µM and 1 mM the peak intensities were 200, 500, 650 and 750 a.u. respectively. The

increase in peak intensity with increase in cadmium ion concentration can be attributed to the attachment of metal ions to the carboxyl groups of GO. Metal ions have Raman enhancing capability. As more ions are attached, the Raman scattering of light increases and thus increasing the Raman peak intensity. Again, the change shows that the GO/AgNWs electrode is responsive to cadmium ions as cadmium ions are attached on the surface of Ag–GO composite.

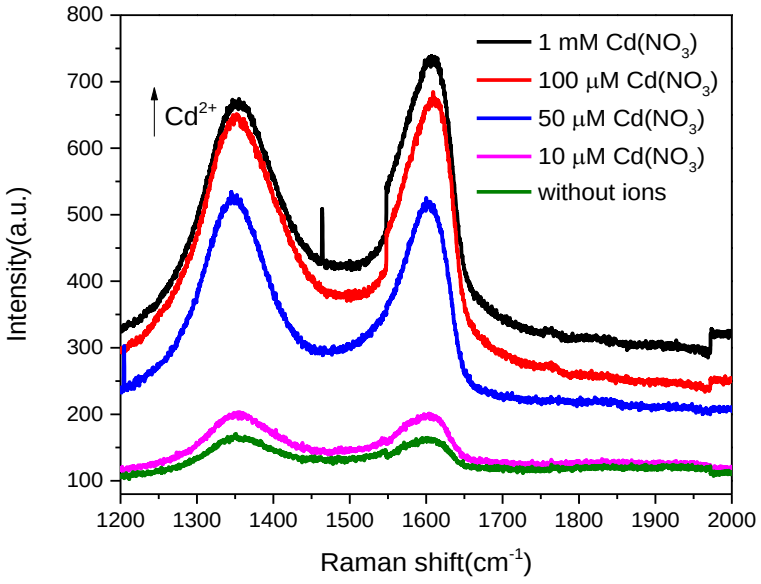

Figure 4. 5 Raman spectra of the GO/AgNWs electrode in response to different concentrations of cadmium ions: 10 µM, 50 µM, 100 µM and 1 mM.

4.3 Cyclic voltammograms for detection of metal ions with GO/AgNWs film

4.3.1 Cyclic voltammetry for mercury chloride to detect mercury ions

Figure 4.6 shows the cyclic voltammogram of GO/AgNWs in response to different concentrations of mercury chloride solutions. The electrolyte was 1:1 mixture of 5 mM $K_4Fe(CN)_6$ and 0.1 M KCl in water. It can be observed that with the increase of mercury

concentration, the intensity of the oxidation peak increased which were found at the potential range of 0.3 - 0.4 V. The sensor surface captures mercury and leads to oxidation and reduction reactions. The more ions the sensor surface captures, the higher the peak redox current intensity.

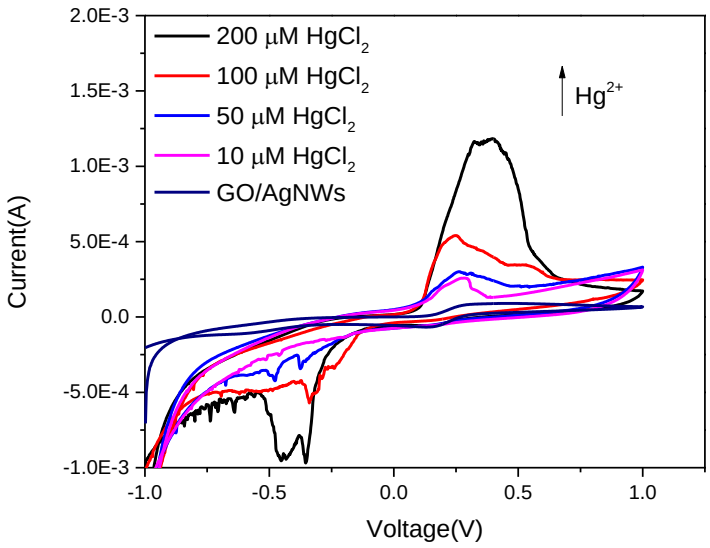

Figure 4. 6 Cyclic voltammograms of GO/AgNWs in response to different concentrations of mercury chloride solutions: 10 µM, 50 µM, 100 µM and 200 µM. The electrolyte was 1:1 mixture of 5 mM $K_4Fe(CN)_6$ and 0.1 M KCl in water.

4.3.2 Cyclic voltammetry for lead iodide to detect lead ions

Figure 4.7 shows the cyclic voltammogram of GO/AgNWs electrode in response to different concentrations of PbI_2 solutions. The electrolyte used was 0.1 M KCl/ $K_4Fe(CN)_6$ in water. It was observed that with the increase of the lead concentration, the intensity of the oxidation peak increased. The oxidation peaks were observed at the potential of 0.2V. The potential is different from the mercury which was at 0.3 to 0.4 V. With the increase in concentration, the sensor surface attaches more lead ions and leads to

more oxidation and reduction reactions. This indicates the good sensitivity of the GO/AgNWs towards lead ions.

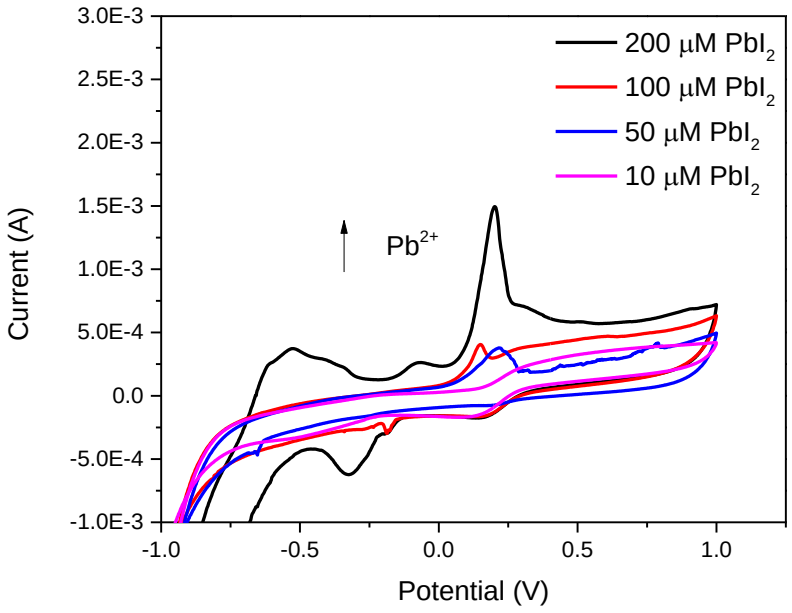

Figure 4. 7 Cyclic voltammograms of GO/AgNWs electrode in response to different concentrations of PbI_2 solutions: 10 µM, 50 µM, 100 µM and 200 µM. Electrolyte 0.1 M KCl/ $K_4Fe(CN)_6$ in water.

4.3.3 Cyclic voltammetry for cadmium nitrate to detect cadmium ions

Figure 4.8 shows the cyclic voltammogram of GO/AgNWs electrode in response to different concentrations of cadmium nitrate to detect cadmium ions. The electrolyte used was 0.1 M KCl/ $K_4Fe(CN)_6$ in water. It was observed that with the increase of cadmium concentration, the intensity of the oxidation peak at ~ 0.6 V increased. The sensor showed a distinct response to cadmium ions with high peak current intensities which indicate the GO/AgNWs sensitivity towards cadmium.

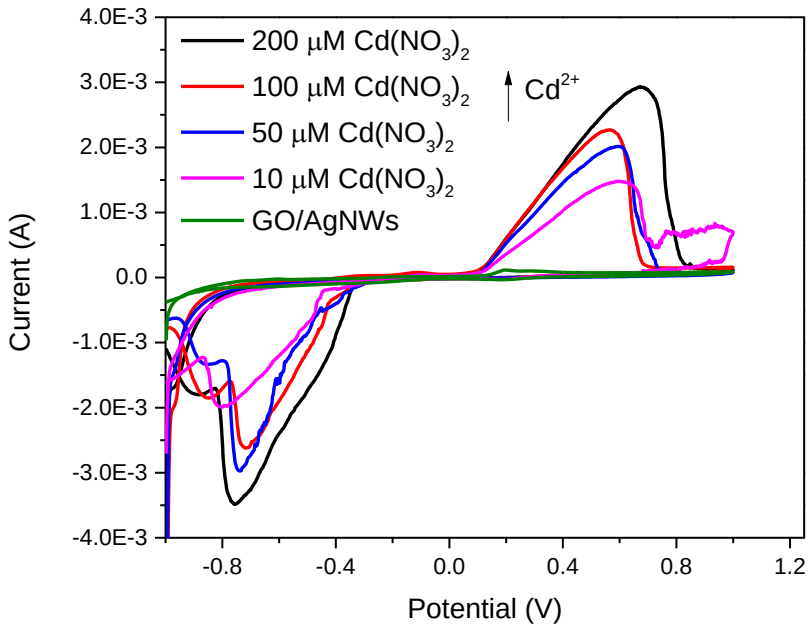

Figure 4. 8 Cyclic voltammograms of GO/AgNWs electrode in response to different concentrations of cadmium nitrate to detect cadmium ions: 10 µM, 50 µM, 100 µM and 200 µM. Electrolyte 0.1 M KCl/ $K_4Fe(CN)_6$ in water.

4.3.4 Linearity of concentration vs. current plot for mercury, lead and cadmium ions

Figure 4.9 shows the current response of the GO/AgNWs electrode to different concentrations of solutions from different metal ions. It was observed that all the different metal ions under investigation depicted linear response but had their own specific range of current response. Lead detection had the least current change of 0-50 µA in response to concentration range of 10 µM-200 µM. Similarly, mercury detection showed a change in current of 25-100 µA for the concentration range of 10 µM-200 µM. Cadmium detection showed the highest current change of 150-300 µA for the concentration range of 10 µM-200 µM. All the three ions under test had oxidation peaks at three different potentials which indicated good selectivity of the sensor. This indicates that the GO/AgNWs can be used to detect all three heavy metal ions simultaneously. The sensitivities were found 7.89

µA/µM, 4.21 µA/µM, 2.63 µA/µM for Cd^{2+}, Hg^{2+}, Pb^{2+} respectively with a detection range was 5 µM - 10 mM. These sensitivities are lower than the previously reported GO/Au nanoparticle electrode sensors. However, the GO/AgNWs sensors have the advantage of lower cost and easily scalable fabrication.

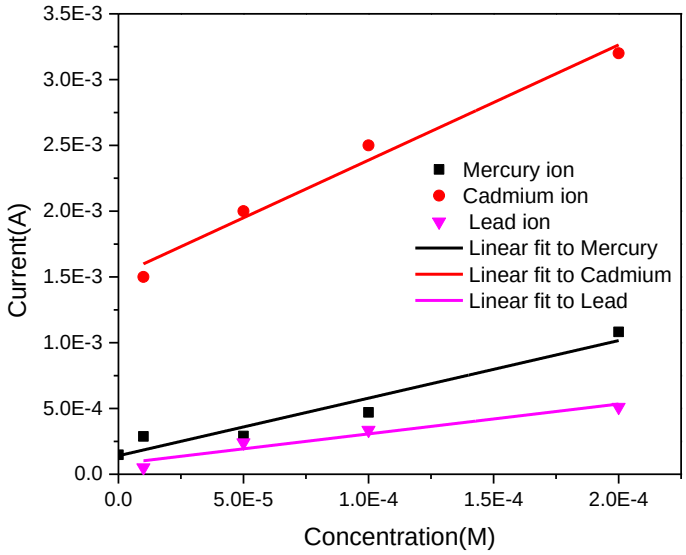

Figure 4. 9 Current response of the GO/AgNWs electrode sensors to different concentrations of solutions from different metal ions.

4.4 SPE for phosphate ion detection in the field soil

4.4.1 Cyclic voltammetry test with and without AgNWs

Figures 4.10 and 4.11 show cyclic voltammograms of SPE electrode for phosphate detection without and with AgNWs, respectively. It can be observed that the use of AgNWs led to an increase in the oxidation current by a factor of 5. The current response range was increased from 0 – 125 µA to 0 – 650 µA. This can be attributed to the increase in surface conductivity of the electrode by AgNWs. The reduction peaks have narrower shapes than the oxidation ones. Reduction peaks can also be selected to measure the concentration change. That is the advantage of cyclic voltammetry that either reaction peaks can be used.

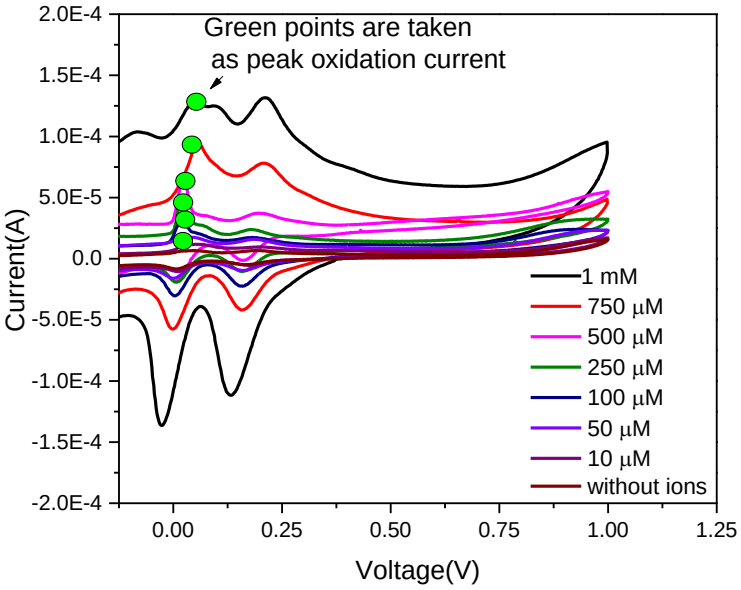

Figure 4. 10 Cyclic voltammograms for phosphate detection without AgNWs.

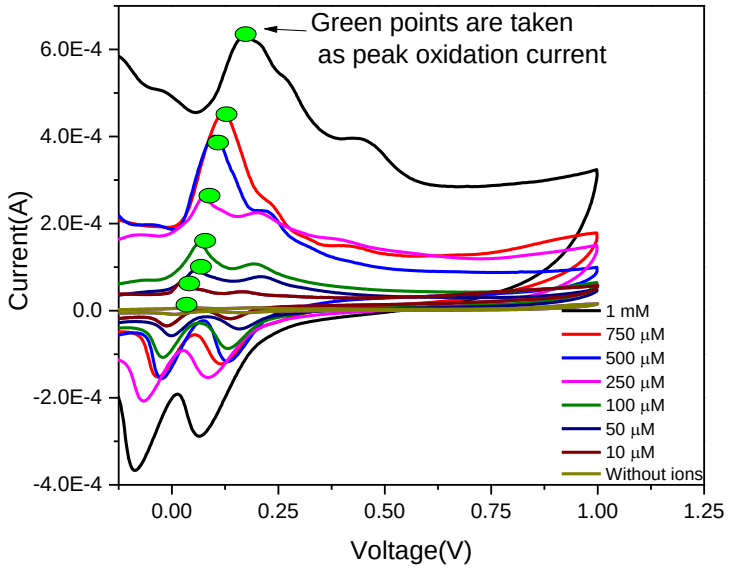

Figure 4. 11 Cyclic voltammograms for phosphate detection with AgNWs.

Figure 4.12 shows linearity of current vs. concentration plot for phosphate detection with and without AgNWs. The oxidation current increased with the increase of concentration as more reaction occurs on AMT modified SPE with AgNWs. The sensitivities of SPE without and with AgNWs were 0.1 µA/µM and 0.71 µA/µM. Therefore, the use of AgNWs increased the sensitivity of the SPE significantly.

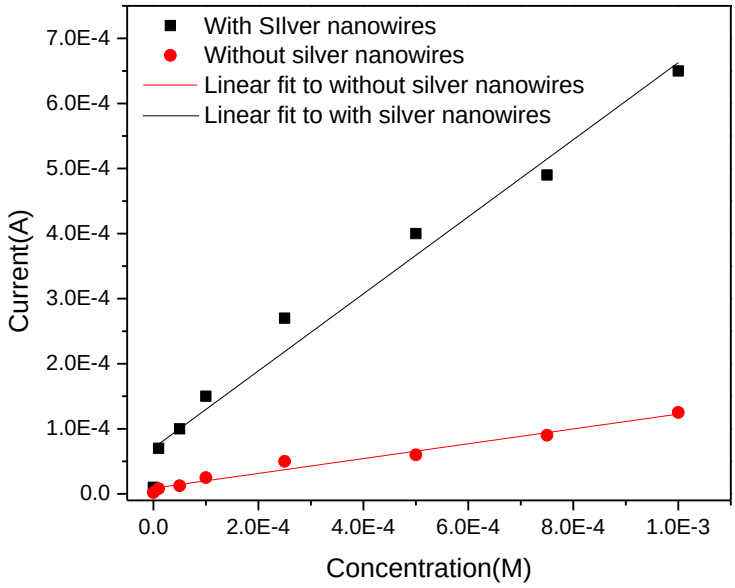

Figure 4. 12 Linearity of current vs. concentration plot for phosphate detection with and without AgNWs.

4.5 Selectivity test with cyclic voltammetry for phosphate detection

Figure 4.13 shows the oxidation peak for the H_2SO_4/KCl electrolyte solution where the working electrode is modified with AMT; the counter electrode is carbon and reference electrode is silver. A single oxidation peak was found at 0.1V potential. Figure 4.14 shows two oxidation peaks for the electrolyte/AMT/phosphate ions. Two oxidation peaks were observed at 0.05V and 0.1V potential. These two oxidation peaks were found due to the two steps of the following oxidation reaction. $Mo_7O_{24}^{6-}$ and H^+ were each oxidized and thus

resulted in two peaks. These peaks are found only in the presence of phosphate ions which indicates the selectivity for phosphate ions.

$$7H_3PO_4 + 12Mo_7O_{24}^{6-} + 51H^+ = 7PMo_{12}O_{40}^{3-} + 36H_2O$$

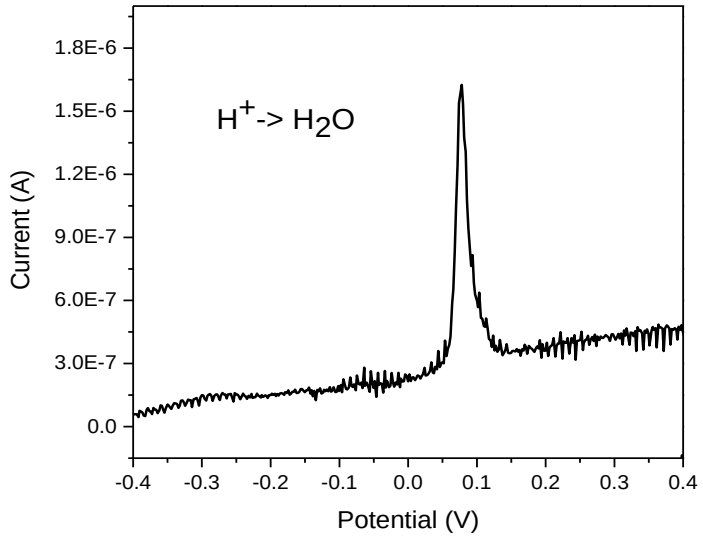

Figure 4. 13 A single oxidation peak for electrolyte solution without phosphate ions where the working electrode is modified with AMT, counter electrode is carbon and reference electrode is silver.

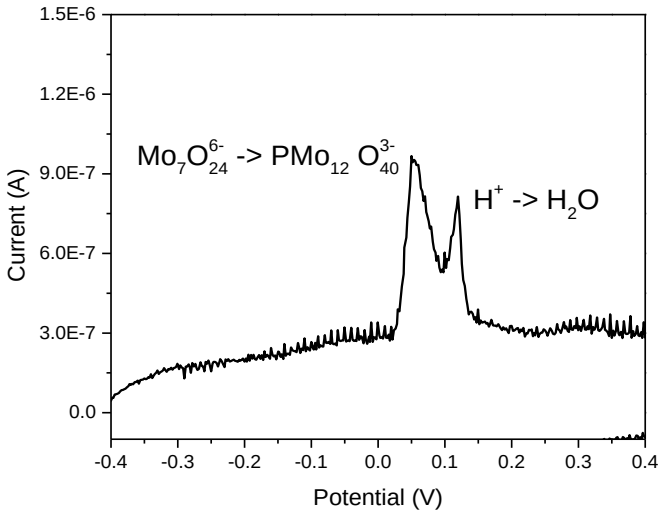

Figure 4. 14 Oxidation peaks for the electrolyte solution/ AMT/phosphate ions.

4.5.1 Repeatability test for modified SPE for phosphate detection

Figure 4.15 shows the repeatable results of cyclic voltammogram measurements of SPE for different concentrations of phosphate ion solution. In the repeatability results, the two peaks were found at the same potential position for each, and the trend of change was same. The current change due to the concentration change also matched the previous experimental data.

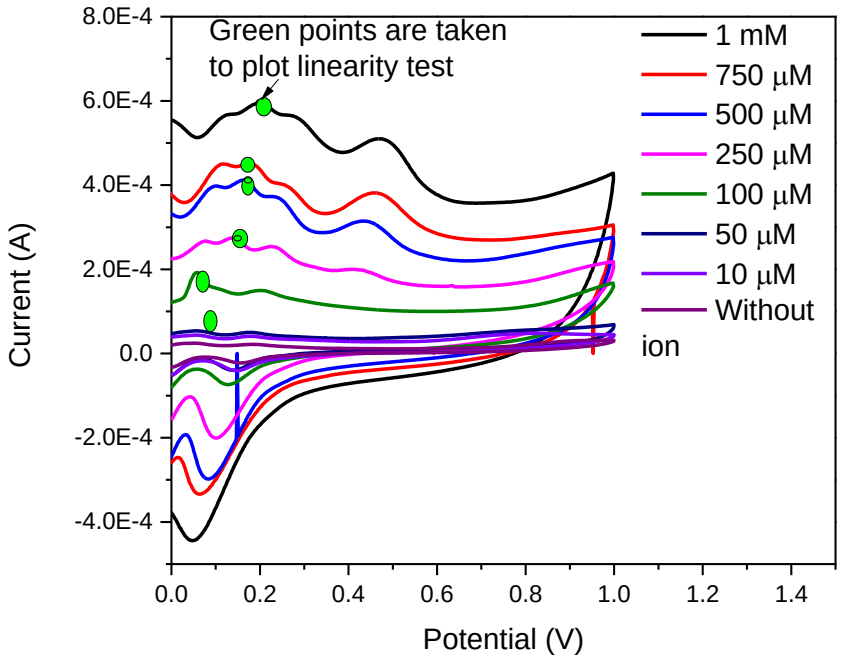

Figure 4. 15 Repeatable results of cyclic voltammogram measurements of SPE for different concentrations of phosphate ion solutions.

Figure 4.16 shows the linearity of current vs. concentration plot for phosphate detection for repeatability test with four different experiments. Table 4.1 summarizes the values of the current change with respect to change in concentration for four different experiments with standard deviation. The linearity of the four experiments almost

overlapped each other which indicated good repeatability and consistency of the device performance.

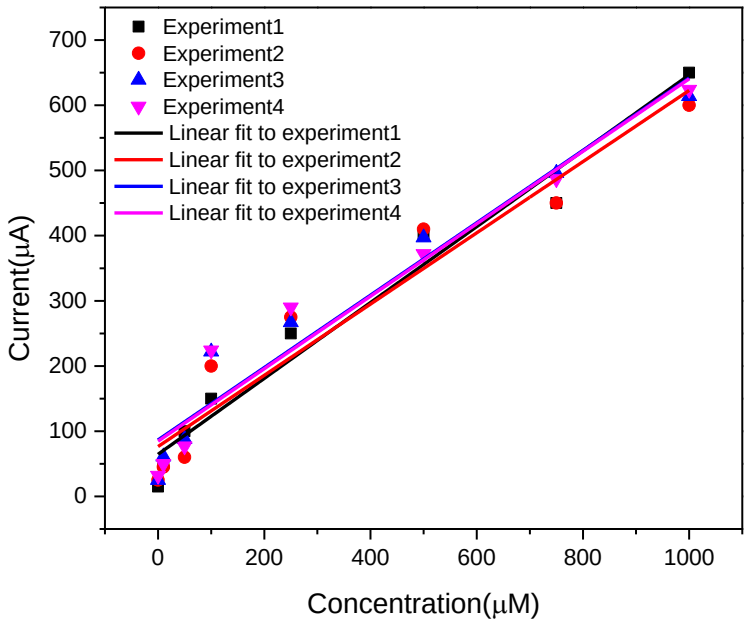

Figure 4. 16 Linearity plot of current vs. concentration for phosphate detection for repeatability test with four different experiments.

Figure 4.17 shows the plots with error bars in terms of standard deviation for different concentration of phosphate ions. The average value and standard deviation were calculated. The least and highest standard deviations were found 5.85 µA and 29.81 µA. The error bars show that there is 5-6% of error prevailing in the measurements which are in the tolerable range. For the phosphate detection, the sensitivity and the detection range were found to be 0.71 µA/µM and 5 µM- 50 mM. It shows better sensing limit than previously reported carbon black modified electrode which was 6 µM.

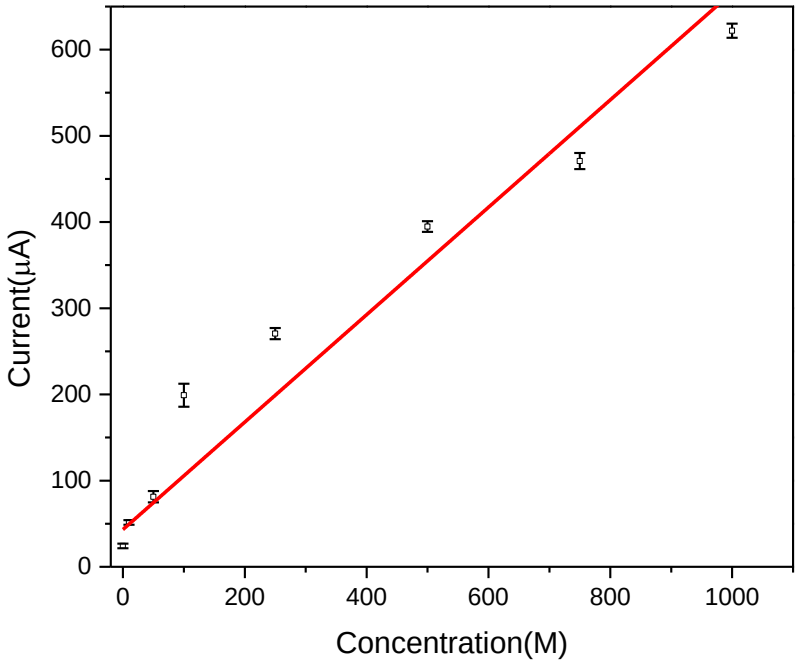

Figure 4. 17 Plots of error bars in terms of standard deviation for different concentrations of phosphate ions.

Table 4. 1 Comparison of current response for different concentration of phosphate ion for four different experiments.

Concentration (µM)	Current1 (µA)	Current2 (µA)	Current3 (µA)	Current4 (µA)	Average Current(µA)	Standard deviation(µA)
1000	650	600	614	624	622	18.27
750	450	450	496	487	470.75	20.99
500	400	410	397	372	394.75	13.98
250	250	275	267	290	270.5	14.43
100	150	200	222	224	199	29.81
50	100	60	88	77	81.25	14.72
10	50	45	61	50	51.5	5.85
0	15	25	25	32	24.25	6.05

4.6 I-V characteristic of SPE for phosphate ion detection

4.6.1 Ion detection using SPE carbon electrode modified with PCBM

Table 4.2 describes current measurement for different ion solutions using modified SPEs with PCBM. The current was determined using I-V measurement. The ions used in

the table are present in a field soil. As can be seen, the SPE showed higher sensitivity towards chloride, phosphate and nitrate ions with higher current intensity for the same concentration of ion solutions. However, this does not provide selectivity.

Table 4. 2 Current measurements for different ion solutions using modified SPE with PCBM

Solution	Concentration	Current(mA)
DI water	---	0.7
NH_4OH	100 mM	1.2
$HgCl_2$	100 mM	1.9
$CdNO_3$	100 mM	2.4
Na_2HPO_4	100 mM	2.7
KCl	100 mM	3.3

4.6.2 Ion detection using SPE carbon electrode modified with ammonium molybdate tetrahydrate

The carbon working electrode was modified with 0.1 M KCl, 0.1 M H_2SO_4, 1 mM AMT. AMT was used as it can react with phosphate ions. Table 4.3 shows current measurement for different ion solutions using modified SPE with ammonium molybdate tetrahydrate. As can be seen, the intensity of the current increased to 8.5 mA for the phosphate ion solution compared to SPE with PCBM at 2.7 mA. This was attributed to the reaction of AMT to phosphate ions.

In addition, the voltage was decreased from 10V to 3V as it is less power consuming. In the field generally only 3V is used. Table 4.4 shows current change measurement with a change in voltage for phosphate detection. It can be observed that for 3V the change is obviously lower than 10V.

Table 4. 3 Current measurements for different ion solutions using modified SPE with ammonium molybdate tetrahydrate

Solution	Concentration	Current(mA)
DI water	---	0.7
NH_4OH	100 mM	1.2
$HgCl_2$	100 mM	1.9
$CdNO_3$	100 mM	2.4
Na_2HPO_4	**100 mM**	**8.5**
KCl	100 mM	3.3

Table 4. 4 Current change measurement with change in voltage for phosphate ion detection

Voltage	Current (with AMT but without phosphate)	Current (with AMT And phosphate)	Increment
10 V	2 mA	8 mA	4 times
3 V	0.245 mA	0.5 mA	2 times

4.6.3 I-V characteristics for SPE at different concentrations of phosphate ions

Figure 4.18 shows the I-V characteristics of the AMT modified SPE without AgNWs for different concentrations of phosphate ion solutions. It can be observed that the current increased with the increase in the concentration of phosphate ions as more electrolysis reactions take place. Figure 4.19 shows the I-V characteristic of the AMT modified SPE with AgNWs for different concentrations of phosphate ion solutions. The similar observation of current increase with increased concentration was observed. However, the current value was increased due to AgNWs. For SPE without AgNWs, the current range is 0.001-0.0018 A while with AgNWs, range is 0.0005-0.004A.

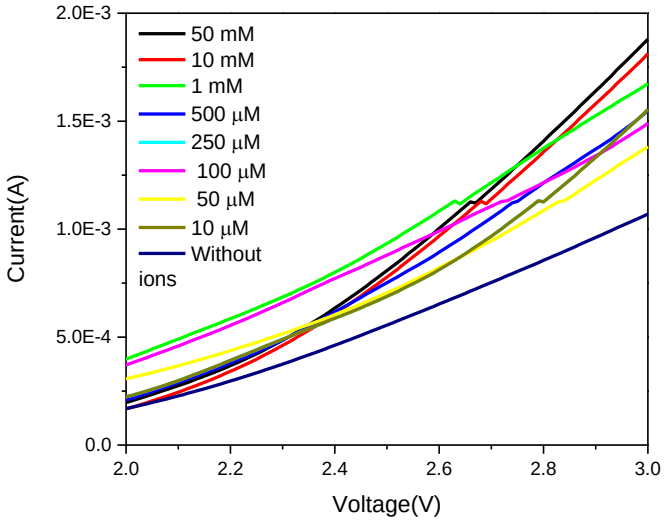

Figure 4. 18 I-V characteristics of AMT modified SPE without AgNWs for different concentrations of phosphate ions.

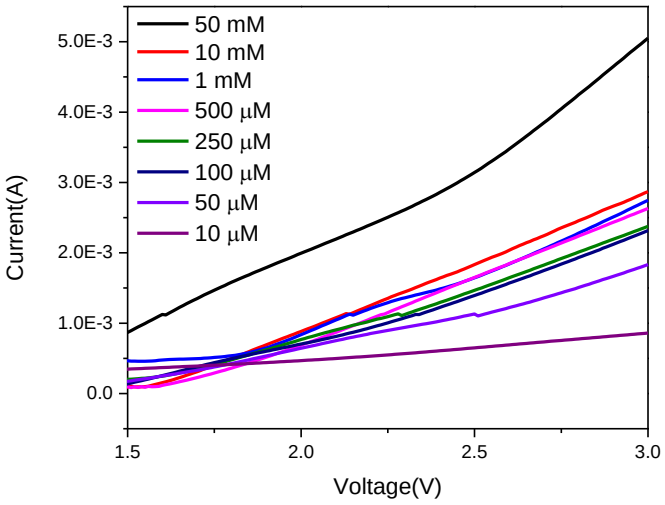

Figure 4. 19 I-V characteristics of AMT modified SPE with AgNWs for different concentrations of phosphate ions.

4.6.4 Resistance change with concentration of phosphate ion solutions

The resistance change of the SPE with respect to the concentration was calculated from I-V curves for both with and without AgNWs and are plotted as shown in figure 4.20. The voltage was 3 V as it has the highest current change. The range for resistance change is from 400 to 2000 Ω for the concentration change from 5 µM to 50 mM for with AgNWs. The sensitivity of the SPE without and with AgNWs was 0.2 Ω/µM and 1.6 Ω/µM respectively. The fitted curve showed a negative linear relation between concentration and resistance. Measurement of resistance needs very less equipment which makes this system portable and field deployable.

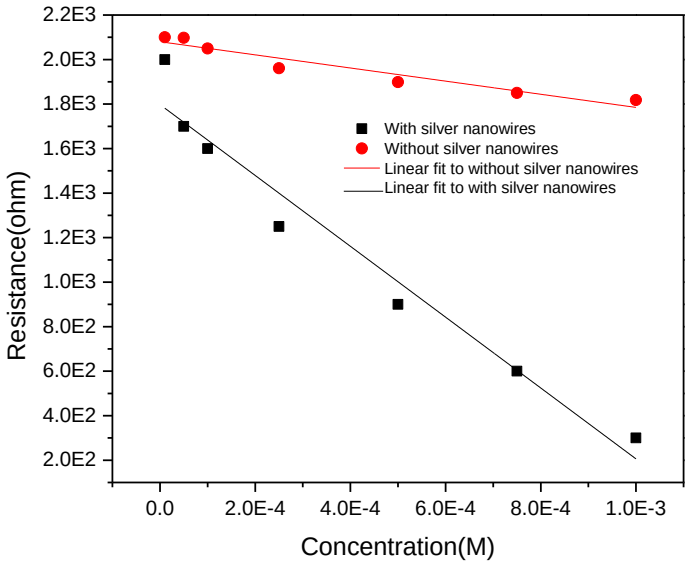

Figure 4. 20 Plot of resistance vs. concentration with and without AgNWs for phosphate ion detection. The resistance was calculated at a voltage of 3V in figure 4.19.

Chapter 5: Conclusions

5.1 Summary

Heavy metals are considered as low-density chemical components which are very toxic. These heavy metals are non-biodegradable, widely dispersed and present serious hazard to human health and environment. The sensing of these ions is one of the most attractive applications due to their large production and toxicity. Phosphorous-containing fertilizer is imperative to plant and animal nutrition as plant growth and growth of essential biomolecules of human body depend upon the proper availability of phosphate ions. The high concentration of heavy metal and phosphate ions in the aquatic system affects the human immune system, permanently damage and/or injuries skin.

Various materials have been employed as sensor electrodes for the detection of heavy metal ions. Carbon-based materials such as graphene, carbon nanotubes, GO have been used to detect metal ions. In addition, metal nanoparticles such as Au, Ag, and Pt have been used in conjunction with carbon-based electrodes to achieve higher electrode conductivity. However, the methods employed were complex, costly and not portable for field deployment. For the detection of phosphate ions, various methods such as colorimetry can be used. However, the colorimetric setup is difficult to adjust for online estimation since it requires plenty of reagents and is ascorbic corrosive. Also, the simple SPE has been used with incorporated sensing materials such as carbon black and pyruvate oxidase. However, these detection systems exhibited poor detection limits with a non-linear response.

There is a need for low cost, portable, repeatable, highly sensitive, highly detection ranged and field deployable sensors to monitor the health of field soil. The goal of this

work was to develop a simple electrochemical sensor using novel GO/AgNWs for heavy metal ions detection and novel modified SPE for phosphate detection to achieve simplicity, high sensitivity, wide detection range, high repeatability and portability. GO is a single layer of carbon atoms with large surface area, high catalytic properties and has oxygen functional groups covalently attached to carbon atoms making it hydrophilic. This makes it suitable for sensing application in biomedical and agriculture areas. AgNWs can be attached by epoxy, carboxyl, hydroxyl, and carbonyl functional groups and adsorbed on the top of GO via the Ag–π orbital connection. These functional groups offer improved electrostatic interface between Ag-GO and negatively charged GO and form an Ag–GO composite. Having oxygen functional groups, metal molecules that are considered as an electron donor can be adsorbed on the plane of GO-AgNWs layer, providing a good detection ability. The easiness of industrial manufacturing of SPE makes it economically feasible for on-site field monitoring and favourably comparable with current portable meters used in the environmental applications.

For the metal ion detection, a solution of AgNWs, GO/AgNWs and different concentrations of metal and phosphate ions were prepared. The sensing electrode GO/AgNWs was fabricated by spin coating onto an FTO glass substrate, and the solution of metal ion of interest was drop casted on top of it. For phosphate detection, the SPE was modified with AgNWs and AMT, and the phosphate solution was drop casted. These electrodes were characterized using Raman, cyclic voltammetry and I-V measurements.

Mercury, lead, cadmium ions had oxidation peaks at three different potentials which indicated good selectivity of the GO/AgNWs sensing electrode sensors. So, this sensor film can be used to detect three different heavy metal ions simultaneously. The

sensitivities of the GO/AgNWs were found to be 7.89 µA/µM, 4.21 µA/µM, 2.63 µA/µM for Cd^{2+}, Hg^{2+}, Pb^{2+} respectively and the detection range was from 5 µM to 10 mM. This sensitivity is lower than the previously reported GO/Au nanoparticle electrode. However, GO/AgNWs has the advantage of lower cost and easily scalable fabrication.

From the cyclic voltammetry measurements, the sensitivity of AMT modified SPE without and with AgNWs were 0.1 µA/µM and 0.71 µA/µM respectively and detection range was 5 µM-50 mM. Therefore, the use of AgNWs increased the sensitivity of the AMT modified SPE significantly. In addition, from the I-V measurements, the sensitivity of the SPE without and with AgNWs were 0.2 Ω/µM and 1.6 Ω/µM respectively depicting a negative linear relation between concentration and resistance. The repeatability tests showed an error of only 5-6%. This Measurement of resistance needs very less equipment which makes this system portable and field deployable.

5.2 **Conclusions**

A novel GO/AgNWs composite film was developed to detect heavy toxic metal ions such as Cd^{2+}, Hg^{2+}, Pb^{2+} and a modified SPE with AMT/AgNWs was invented to detect phosphate ions in water solution. GO/AgNWs films showed a sensitivity of 7.89 µA/µM, 4.21 µA/µM, 2.63 µA/µM for Cd^{2+}, Hg^{2+}, Pb^{2+} ions, respectively. The existence of oxidation peaks at different potentials for different metal ions demonstrated good selectivity of the GO/AgNWs electrode. The modified SPE sensors demonstrated repeatable sensitivity of 0.71 µA/µM and a wide detection range 5 µM-50 mM with a small error of 5-6%.

Heavy metal and phosphate ion sensors are not commercially well cost effective. Some of them are very expensive and complicated to manufacture, and bulky instruments are needed to obtain results. The sensing electrode based sensors developed in this work can be a potential simple and low cost system owing to the easy fabrication process and use of cheaper materials. They are also portable as they are small and need less equipment to collect data for field deployment. However, the sensitivity still requires improvement.

5.3 **Future work**

Future work includes the use of the developed GO/AgNWs electrode and AMT/AgNWs modified SPE sensors for microcontroller based real time monitoring sensing systems for heavy metal ions and phosphorous-containing species with Global Positioning System (GPS) in the agricultural fields. Modification of the electrode surface with different noble biomaterials such as DNA, protein, antibody, etc. can be carried out to address film sensitivity and detection range.

References:

1. Zhang, M., et al., *Recent advances in the synthesis and applications of graphene–polymer nanocomposites.* Polymer Chemistry, 2015. **6**(34): p. 6107-6124.
2. Gumpu, M.B., et al., *A review on detection of heavy metal ions in water–An electrochemical approach.* Sensors and Actuators B: Chemical, 2015. **213**: p. 515-533.
3. Minnesota Pollution Control Agency • 520 Lafayette Rd. N., S.P., MN 55155-4194 *Importance of phosphate*. Available from: https://www.pca.state.mn.us/sites/default/files/wq-iw3-22.pdf.
4. agriculture, S.D.d.o.; Available from: https://sdda.sd.gov/office-of-the-secretary/agriculture-industry/.
5. Tacio, D.H.a.H.; Available from: https://www.wilsoncenter.org/sites/default/files/popwawa2.pdf.
6. Cinti, S., et al., *Novel reagentless paper-based screen-printed electrochemical sensor to detect phosphate.* Analytica chimica acta, 2016. **919**: p. 78-84.
7. Adeloju, S.B., *Progress and recent advances in phosphate sensors: A review.* Talanta, 2013. **114**: p. 191-203.
8. Stradiotto, N.R., H. Yamanaka, and M.V.B. Zanoni, *Electrochemical sensors: a powerful tool in analytical chemistry.* Journal of the Brazilian Chemical Society, 2003. **14**(2): p. 159-173.
9. Freiser, H., *Ion-selective electrodes in analytical chemistry*. 2012: Springer Science & Business Media.
10. Kelly, R.G. and A.E. Owen, *Solid-state ion sensors. Theoretical and practical issues.* Journal of the Chemical Society, Faraday Transactions 1: Physical Chemistry in Condensed Phases, 1986. **82**(4): p. 1195-1208.
11. Hayat, A. and J.L. Marty, *Disposable screen printed electrochemical sensors: Tools for environmental monitoring.* Sensors, 2014. **14**(6): p. 10432-10453.
12. Kavinkumar, T. and S. Manivannan, *Uniform decoration of silver nanoparticle on exfoliated graphene oxide sheets and its ammonia gas detection.* Ceramics International, 2016. **42**(1): p. 1769-1776.
13. Tang, S., et al., *Label free electrochemical sensor for Pb 2+ based on graphene oxide mediated deposition of silver nanoparticles.* Electrochimica Acta, 2016. **187**: p. 286-292.
14. Promphet, N., et al., *An electrochemical sensor based on graphene/polyaniline/polystyrene nanoporous fibers modified electrode for simultaneous determination of lead and cadmium.* Sensors and Actuators B: Chemical, 2015. **207**: p. 526-534.
15. Gnanaprakasam, P., et al., *Simple and Robust Green Synthesis of Au NPs on Reduced Graphene Oxide for the Simultaneous Detection of Toxic Heavy Metal Ions and Bioremediation Using Bacterium as the Scavenger.* Electroanalysis, 2016. **28**(8): p. 1885-1893.
16. Some, S., et al., *Highly sensitive and selective gas sensor using hydrophilic and hydrophobic graphenes.* Scientific reports, 2013. **3**: p. 1868.

17. Cui, S., et al., *Controllable synthesis of silver nanoparticle-decorated reduced graphene oxide hybrids for ammonia detection.* Analyst, 2013. **138**(10): p. 2877-2882.
18. Liang, J., et al., *Silver nanowire percolation network soldered with graphene oxide at room temperature and its application for fully stretchable polymer light-emitting diodes.* Acs Nano, 2014. **8**(2): p. 1590-1600.
19. Talarico, D., et al., *Phosphate detection through a cost-effective carbon black nanoparticle-modified screen-printed electrode embedded in a continuous flow system.* Environmental science & technology, 2015. **49**(13): p. 7934-7939.
20. Gilbert, L., et al., *Development of an amperometric assay for phosphate ions in urine based on a chemically modified screen-printed carbon electrode.* Analytical biochemistry, 2009. **393**(2): p. 242-247.
21. Bard, A.J.P., Roger; and Jordan, Joseph, eds. (1985). *Electrochemistry*. Available from: http://www.chemistryexplained.com/Di-Fa/Electrochemistry.html.
22. Champake Mendis, M., PhD. *Oxidation and reduction in electrochemistry*. Available from: https://drushapchem.wikispaces.com/%E2%80%A2+Electrochemistry.
23. Li, J., T. Peng, and Y. Peng, *A cholesterol biosensor based on entrapment of cholesterol oxidase in a silicic sol-gel matrix at a prussian blue modified electrode.* Electroanalysis, 2003. **15**(12): p. 1031-1037.
24. Mabbott, G.A., *An introduction to cyclic voltammetry.* J. Chem. Educ, 1983. **60**(9): p. 697.
25. scientific, H. *Raman Spectroscopy Theory*. Available from: http://www.horiba.com/scientific/products/raman-spectroscopy/raman-academy/raman-tutorial/the-theory-of-raman-spectroscopy/.
26. Holly J Butler, L.A., Benjamin Bird, Gianfelice Cinque, Kelly Curtis, Jennifer Dorney, Karen Esmonde-White, Nigel J Fullwood, Benjamin Gardner, Pierre L Martin-Hirsch,Michael J Walsh, Martin R McAinsh, Nicholas Stone & Francis L Martin. *Schematic diagram of Raman scattering*. Available from: http://www.nature.com/nprot/journal/v11/n4/full/nprot.2016.036.html?WT.feed_name=subjects_raman-spectroscopy.
27. Susan Swapp, U.o.W. *Principle of Scannong Electron Microscope*. Available from: http://serc.carleton.edu/research_education/geochemsheets/techniques/SEM.html.
28. Jim Schweitzer, P.U., West Lafayette, IN 47907, (765) 494-4600 © 2014 Purdue University. *Image of Scanning Electron Microscope*. Available from: https://www.purdue.edu/ehps/rem/rs/sem.htm.